Annu. Rev. Nutr. 1997. 17:559–96

APPLICATIONS OF MASS ISOTOPOMER ANALYSIS TO NUTRITION RESEARCH

Henri Brunengraber
Department of Nutrition, Case Western Reserve University, Cleveland, Ohio 44106; e-mail: hxb8@po.cwru.edu

Joanne K. Kelleher
Department of Physiology, George Washington University, Washington, DC 20037

Christine Des Rosiers
Department of Nutrition, Université de Montréal, Montréal QC, H3C 3J7, Canada

KEY WORDS: nutrient metabolism, intermediary metabolism, metabolic regulation, tracer methodology, stable isotopes

ABSTRACT

Investigations into regulating metabolic pathways with stable isotopes have, over the past decade, undergone major development with the use of nuclear magnetic resonance and mass spectrometry in studying labeling patterns of newly synthesized biomolecules. In this review, we concentrate on investigations of mass isotopomer distribution (MID) measured by mass spectrometry. We review the applications of MID to analytical problems, in particular the possibility of amplifying the measurement of low isotopic enrichments by incorporating multiple molecules or atoms of a primary analyte into the molecule of a secondary analyte, the MID of which is assayed. We also review new information on the regulation of intermediary metabolism gathered from the analysis of MID patterns of synthesized compounds. Lastly, we review the applications of MID to the synthesis of polymeric molecules, with emphasis on the validity of these techniques. A number of these techniques are applicable to investigations of nutrient metabolism in health and disease.

CONTENTS

0199-9885/97/0715-0559$08.00

DEFINITIONS

During the past decade we have witnessed an explosion of research on the biosynthesis of molecules containing multiple stable isotopic atoms. This is a review on the applications of such research. In it, we consider only molecules with different distributions of the stable isotopes ^{13}C, ^{2}H, ^{15}N, and ^{18}O. The concepts outlined below, however, can be applied to other types of atoms, stable or radioactive. Because of the low proportions of ^{13}C (1.10%), ^{2}H (0.015%), ^{15}N (0.37%), and ^{18}O (0.20%) in the natural elements, labeled molecules are identified by the number and position(s) of heavy isotopes in their constitutive atoms.

There are no strict IUPAC guidelines regarding the nomenclature used to describe multiply labeled molecules. Correspondence between nomenclatures based on strict chemical definition and on biological usage is, respectively:

isotopolog and mass isotopomer, isotopomer and positional isotopomer, and isotopolog or isotopomer and isotopomer. In this review, we use the nomenclature followed by most biological investigators, although it may not be fully correct (119). According to the biological usage, there are two types of isotopomers. Positional isotopomers have identical global isotopic composition but differ by the position of the heavy atoms in the molecule. For example, [1-^{13}C]glucose and [2-^{13}C]glucose are positional isotopomers. So are [1,2,3,4-$^{13}C_4$]octanoate and [5,6,7,8-$^{13}C_4$]octanoate. Mass isotopomers differ by the number of heavy atoms in their molecules, resulting in different molecular weights. For example, [$^{14}N_2$]urea, [^{14}N-^{15}N]urea, and [$^{15}N_2$]urea are mass isotopomers. Usually, the lightest atoms are not specified and these mass isotopomers are identified as urea, [$^{15}N_1$]urea, and [$^{15}N_2$]urea, in agreement with the International Union of Chemistry. In mass spectrometric jargon, they are referred to as (M), (M + 1), and (M + 2) urea, or—as used in this review—as M, M1, and M2 urea.

A given isotopomeric mass may correspond to molecules with different types of heavy atoms: [^{13}C]urea and [$^{15}N_1$] urea are both M1 isotopomers. Similarly, [^{13}C-$^{15}N_1$]urea and [$^{15}N_2$]urea are both M2 isotopomers. When only one element of a compound with n such atoms is labeled, the number of possible mass isotopomers is $(n + 1)$ and the number of positional isotopomers of all masses is 2^n. For example, glucose has seven possible ^{13}C-labeled mass isotopomers and 64 positional isotopomers. Most mass isotopomers of glucose, except M and M6, include multiple positional isotopomers. The number of positional isotopomers of symmetrical molecules (succinate) or radicals (methyl) is less than 2^n. However, chemically symmetrical molecules may be biologically asymmetrical because of (*a*) the configuration of the active site of enzymes (e.g. the citrate synthase and lyases) or (*b*) metabolic channeling.

MEASUREMENTS OF MASS ISOTOPOMER DISTRIBUTION

Technical Considerations

Mass spectrometry allows measurement of the mass distribution of molecules or molecular fragments. Masses are usually measured with a precision of 0.1 atomic mass units (AMU). This is adequate for most applications, but it will not resolve signals from compound pairs such as [^{13}C-$^{15}N_1$]urea and [$^{15}N_2$]urea. Such separation is difficult even with a high-resolution instrument.

Usually, mass isotopomer distribution (MID) analysis associates capillary gas chromatography (GC) or high-pressure liquid chromatography (HPLC) to

mass spectrometry (MS). A long capillary GC column (10–50 m) minimizes the interference of unknown compounds that coelute with the analyte and that yield ions in the mass range observed by selective ion monitoring. This interference, which does not usually occur with standards, occurs quite frequently—especially with HPLC-MS—when the analyte is assayed in a complex matrix such as tissue homogenate or urine and/or the retention time of the analyte is short. The consequence of such interference is an erroneous MID of the labeled analyte. One can test for such interference by analyzing a baseline unlabeled sample and monitoring the natural MID of the analyte's ion cluster. This MID should be identical to the theoretical MID and to that measured with a pure standard.

Prevention of interference may require purification of the compound before analysis, testing various types of column of increasing length, and adjusting the temperature program of the GC so that the analyte elutes after a long time, sometimes up to 1 h (28). One should never consider an interference detected in a baseline unlabeled sample as a constant background that can be safely deducted from the MID measured in a subsequent labeled sample. The same considerations apply to simple isotope dilution assays and to measurements of isotopic enrichment at one mass.

Many compounds require derivatization before GC-MS analysis. Derivatizing groups include atoms (C, N, Si, B) with a natural abundance of heavy isotope(s), which increase the mole fractions of heavy isotopomers of the naturally labeled analyte. This effect often decreases the precision of measurements of the low proportion of heavy isotopomers formed during some biological experiments. To minimize this problem, one can (*a*) use small derivatizing groups without Si or B, (*b*) use derivatizing groups that are either fully ^{13}C-labeled or ^{13}C-depleted, or (*c*) use derivatizing groups that split off in the mass spectrometer.

Consider for example the measurement of a low ^{2}H enrichment on carbon 2 (C2) of glucose in humans whose body water was 0.5% enriched with $^{2}H_2O$ (74, 75). One can convert glucose to sorbitol and enzymatically transfer the H on C2 to pyruvate. This forms [2-^{2}H]lactate, which is assayed as the *n*-propylamide heptafluorobutyrate derivative with a baseline M1/M enrichment of 8.5% (75). Alternatively, the H is transferred to [U-$^{13}C_3$]pyruvate, forming [U-$^{13}C_3$, 2-^{2}H]lactate, which is assayed as the pentafluorobenzyl derivative by negative chemical ionization GC-MS (43). Because the pentafluorobenzyl group splits off in the ion source (42), the [U-$^{13}C_3$, 2-^{2}H]lactyl ion has a baseline M4/M3 enrichment of only 0.5%. This allows the measurement of ^{2}H enrichment on C2 of glucose down to 0.1% (43).

The precision of MID measurement can also be increased by combining multiple molecules or atoms of the analyte into a larger molecule (see below).

Consideration of Natural Enrichment in Measured MID

Investigators are well aware that studies involving isotopes with a significant natural abundance must account for the effect of these naturally occurring isotopes when estimating the incorporation of labeled substrates into products. A common approach to this problem has been to correct the observed isotopomer profile for the natural abundance of significant isotopes prior to estimating the incorporation of the labeled substrate. This approach involves a two-step process: Data is corrected for natural abundance, then the corrected isotopomer distribution is used to obtain estimates of parameters related to biosynthesis.

For molecules that are multiply labeled with atoms of nonnegligible natural enrichment (^{13}C, ^{15}N), correction of the measured MID of a biologically labeled sample for natural enrichment MID is more complicated than simple subtraction of mole fractions at each mass. Rosenblatt et al (114) have pointed out the skew of natural abundance MID when increasing numbers of C or N atoms become labeled. Once an atom is fully labeled, it no longer has a natural enrichment. So, simple subtraction of baseline MID from labeled MID leads to overcorrections and artifactually negative mole fractions for some mass isotopomers (39).

Three types of computation are used to deduct the natural MID from the measured labeled MID. First, a series of enrichment calibration curves can be constructed when standards of increasingly labeled compounds are available (39, 107). For example, the MID of pyruvate containing M, M1, M2, and M3 isotopomers can be corrected for natural enrichment by using four calibration curves constructed by running samples of unlabeled, [3-^{13}C], [2,3-$^{13}C_2$], and [U-$^{13}C_3$]pyruvate. This complicated procedure lends itself to propagation of errors. In addition, labeled standards are almost never 100% labeled, and series of increasingly labeled standard (such as M to M6 glucose) are seldom available.

Second, one can use theoretical curves of ratios of mass isotopomer abundance that include baseline enrichment at all masses of interest. However, this technique assumes that the natural MID of the baseline unlabeled sample is absolutely identical to the theoretical MID. This is seldom the case.

Third, computation techniques for correcting the measured MID of multilabeled compounds for baseline MID have been described by Rosenblatt et al (114) and Fernandez et al (39). These techniques take into account any discrepancy between the theoretical and measured baseline MIDs. With the corrected isotopomer profile in hand, the investigator can then proceed to the second step and assess the incorporation of the labeled substrate without interference from the natural abundance of the isotope.

While correcting the isotopomer profile before solving for the parameters is intuitively attractive, there is an alternative, which is to include the natural abundance in the fitting routine (67). This results in a one-step process. The

rationale for this approach is that it is preferable in any modeling procedure to manipulate the data as little as possible before applying the process of parameter estimation. This concept applies only when the number of isotopomers measured exceeds the number of parameters to be estimated. Only under these conditions can errors in the data be noticed.

To illustrate the one-step process, consider a system in which isotopomers are in excess (overdetermined system) and no single solution provides a perfect fit to the data. The fitting routine must decide which isotopomers are in error and by how much. Consider the situation in which the fitting routine decides that the apparent percentage of a given isotopomer, Mi, as measured is higher by 5% than the fit of the data to this model. If the 5% excess in Mi results from an interfering contaminant, it would not be appropriate to use the amount of the 5% excess in the correction routine for natural abundance, since the 5% does not represent the ion of interest. When a precise estimate of the amount of the Mi + 1 isotopomer is important and Mi $\gg$ Mi + 1, this effect can be significant. It is possible to address this issue only if the correction and parameter estimation process are performed simultaneously, as a one-step process. The strength and weaknesses of the various correction methods must be considered by the investigators in the context of their specific experiments.

APPLICATIONS OF MASS ISOTOPOMER DISTRIBUTION TO ANALYTICAL PROBLEMS

Principles

The measurement of the stable isotopic enrichment or concentration of a compound by isotope dilution analysis is usually conducted by monitoring the mass spectrometer signal at two or three masses. Numerous examples of such assays have been published (128). To increase sensitivity and precision of measurements of low concentrations and enrichments, a new type of isotope dilution assay can be conducted by incorporating multiple molecules of a primary analyte into the molecule of a secondary analyte, the MID of which is assayed by GC-MS. The principle of this MID-based approach is as follows:

Consider a primary analyte A that can react with an appropriate reagent B to form a secondary analyte A_nB_m, the molecule of which contains n molecules of A:

$$n\mathrm{A} + m\mathrm{B} \rightarrow A_n\mathrm{B}_m \qquad 1.$$

In the case of a simple polymerization of A, $m = 0$ and the secondary analyte is simply the polymer A_n. As an example, formaldehyde reacts with ammonia

to form hexamethylenetetramine (HMT):

$$6CH_2O + 4NH_3 \rightarrow 6C_6H_{12}N_4 + 6H_2O \qquad 2.$$

Now, suppose A is enriched with its isotopomer A* labeled with one atom (^{13}C, ^{2}H, or ^{15}N) that increases the molecular weight of A by one AMU. The molecules of A_nB_m contain from zero to n A* atoms, depending on the enrichment of the primary analyte. The MID of A_nB_m, after deduction of any natural enrichment, is characterized by a distribution of $n + 1$ mass isotopomers, the frequencies of which can be predicted by probability analysis. In the absence of isotopic effects during the formation of A_nB_m, the MID of the latter is calculated as

$$M_i = \frac{n!}{(i! \times (n-i)!)} \times (F_{A^*})^i \times (F_A)^{(n-i)}, \qquad 3.$$

where M_i is the mole fraction of the ith mass isotopomer of A_nB_m; F_A and F_{A^*} are the mole fractions of A and A*, respectively; i varies from 0 to n. Note that when labeling of A increases its molecular weight by two daltons (if A is labeled with ^{18}O, or with two ^{2}H atoms as in $C[^2H_2]O$), i equals 0, 2, 4, . . . $2n$. The frequency of heavy isotopomers in the MID of A_nB_m increases with the enrichment of A. This is illustrated in Figure 1, which shows the theoretical distribution of the seven hexamethylenetetramine (HMT) mass isotopomers made by reacting [^{13}C]formaldehyde of increasing enrichment with unlabeled NH_3. The symbols refer to the measured MID of HMT made from six samples of formaldehyde with various ^{13}C enrichment. Note that the symbols fall on, or very close to, the theoretical curves.

Assay of the Enrichment of an Analyte

From the measured MID of A_nB_m of a sample containing both A and A*, the mole fraction of A* (F_{A^*}) is calculated from Equation 4, and that of A (F_A) is calculated from $1 - F_{A^*}$.

$$F_{A^*} = \frac{\sum_{i=1}^{n} i \times M_i}{n}. \qquad 4.$$

Plotting the measured F_{A^*} as a function of the theoretical enrichment of the primary analyte A yields a linear calibration curve that can be used to assay the unknown enrichment of other samples.

Assay of the Concentration of an Unlabeled Analyte

As in a classical isotope dilution assay, a calibration curve of concentration is constructed by spiking increasing amounts of pure A with a constant amount of A* before making A_nB_m. The MID of the A_nB_m standards are used to calculate F_{A^*} and F_A for each standard. A linear calibration curve is drawn by plotting

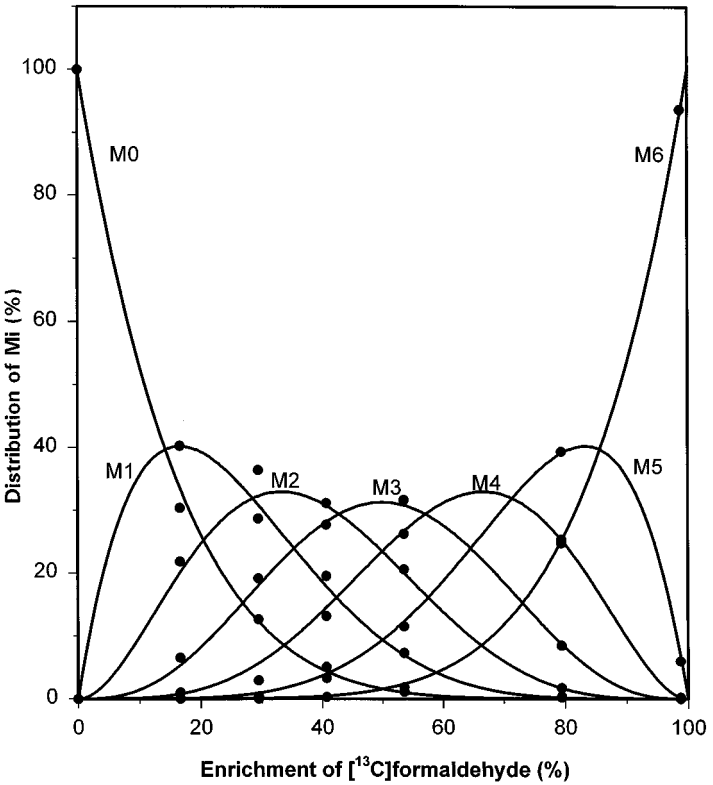

Figure 1 Distribution of the M to M6 mass isotopomers of hexamethylenetetramine (HMT) prepared from samples of [^{13}C]formaldehyde of various enrichments. The continuous lines are the theoretical distributions calculated from Equation 3. Each set of symbols represents the measured MID of a sample of HMT made from a lot of formaldehyde of specific enrichment.

the ratio F_A/F_{A^*} as a function of the amount of unlabeled A. In parallel, samples containing unknown concentrations of A are spiked with the same amount of A^* as the standards are before conversion to A_nB_m and MID analysis. From the calculated ratio F_A/F_{A^*} of the unknowns and the calibration curve, one calculates the concentration of the unknown samples of A.

Assay of the Enrichment and Concentration of an Analyte

Assay of the enrichment and concentration of an analyte requires two parallel assays of the same sample. First, the basal mole fraction in A (F_{A1}) and A^* (F_{A1^*}) is determined as above. Second, the sample is spiked with z nmol or mmol of A^* before forming A_nB_m, MID analysis, and calculation of modified

mole fractions F_{A2} and F_{A2^*}. The original amount of labeled analyte, i.e. $A + A^*$, is calculated by

$$A + A^* = z \times \frac{F_{A2}}{F_{A1} - F_{A2}}. \quad 5.$$

Examples of Analytical Procedures Based on MID

ASSAYS INVOLVING HMT Formed from the condensation of formaldehyde and ammonia in alkaline medium (Equation 2), HMT can be used to assay the labeling of formaldehyde, ammonia, or precursors of these compounds (43, 74, 75, 112, 131)

Assay of the ^2H enrichment on C6 and C2 of glucose The first of the HMT-based assays was described by Landau et al (75), who measured rates of gluconeogenesis (GNG) in humans whose body water had been 0.5% enriched with ^2H by ingesting ^2H_2O. The contribution of GNG to glucose production is equal to the ^2H-labeling ratio in carbons 6 and 2 of glucose (C6/C2). To measure the ^2H enrichment on C6, glucose is oxidized with periodate. This yields formaldehyde, which carries the two H of C6 of glucose (only one of them is labeled). Formaldehyde is reacted with ammonia, forming HMT the M1 enrichment of which is close to six times that of the ^2H on C6 of glucose. The ^2H enrichment on C2 of glucose can also be measured via HMT after converting glucose to a mixture of ribitol-5-phosphate and arabitol-5-phosphate before periodate oxidation (74).

Measurement of glucose turnover in large animals The turnover of glucose is conveniently measured by infusing [6,6-$^2H_2$]glucose and measuring the enrichment of glucose in plasma. In large animals, the prohibitive cost of the tracer can be decreased by assaying the M2 enrichment on C6 of glucose via HMT. In this case, formaldehyde derived from C6 of glucose is doubly labeled. Thus the amplified M2 enrichment of HMT is measured above a low natural M2 enrichment of 0.41%. One can reliably measure M2 enrichments of glucose down to 0.05% (43).

Assay of the concentration and ^{15}N enrichment of plasma ammonium Because of the low concentration of plasma NH_4^+, its ^{15}N enrichment is difficult to measure. The classical technique involves converting NH_4^+ from 10 ml of plasma to N_2 and isotope ratio mass spectrometry (IRMS) analysis. A recent technique involves the enzymatic transfer of NH_4^+ to 2-ketocaproate or to α-ketoglutarate, forming norvaline or glutamate, which are assayed by GC-MS (104, 105). Since the natural M1 enrichment of the ions monitored are 6% and 17%, respectively, measurements of low enrichments of plasma NH_4^+ are imprecise. By using the strategy outlined above, plasma NH_4^+ can be

converted to HMT with formaldehyde, then assayed by GC-MS (131). This multiplies by four the enrichment of NH_4^+. Similarly, low enrichments of L-[5-^{15}N]glutamine or urea can be measured by treatment of an NH_4^+-depleted sample with glutaminase or urease, respectively, followed by HMT formation.

ASSAY OF THE ^{2}H ENRICHMENT OF WATER When GNG or lipogenesis is measured in vivo by enriching body water with ^{2}H, one needs to measure the enrichment of water. This is usually done by reducing water to hydrogen, which is assayed by IRMS. Alternatively, enrichment of ^{2}H in water as low as 0.005% can be measured reliably by a MID-based GC-MS assay (15). This requires incubating the alkalinized water sample with an organic compound containing a ketone or aldehyde group. At high pH, via keto-enol tautomerism, the hydrogens on carbon atoms adjacent to the carbonyl exchange and reach isotopic equilibrium with the hydrogens of water (30, 97). For example, if one incubates acetone with alkaline ^{2}H-enriched water, the MID of acetone shows an increase in the M1 isotopomer that is close to six times the ^{2}H enrichment of water. To decrease the natural M1/M enrichment of acetone (3.5%), one can use [U-$^{13}C_3$]acetone, which has a basal M4/M3 enrichment of only 0.2% (15).

USE OF MASS ISOTOPOMER DISTRIBUTION TO STUDY PATHWAYS OF NUTRIENT METABOLISM

This section reviews studies in which unique information on the mechanisms and regulation of metabolic pathways was gained by MID analysis of tracer(s) and/or product(s). We do not review the numerous reports on the use of single or multiple mass isotopomers to measure substrate kinetics and/or concentrations by isotope dilution (see 128 for review). Studies are presented in order of increasing complexity with respect to data interpretation. Uses of MID to study the synthesis of polymeric molecules are presented below.

In Vivo Formation of Oxysterols

Oxysterols derived from cholesterol oxidation have been implicated in the genesis of atherosclerotic lesions. However, cholesterol oxidation can occur in vivo and during in vitro sample processing. To clarify the origin of oxysterols, Breuer & Bjorkhelm (12) exposed live rats for a few hours to air containing $^{18}O_2$. After flushing out $^{18}O_2$, the rats were sacrificed and sterols were analyzed by GC-MS. Oxysterols enriched with M2 and M4 isotopomers could only be formed in vivo from preformed and newly synthesized cholesterol, respectively. In contrast, unlabeled oxysterols are likely to be of dietary origin or artifacts produced in vitro.

Gluconeogenic Potential of Dicarboxylic Acids

Dicarboxylic acids arise from the minor pathway of ω-oxidation of long-chain fatty acids. In subjects with inborn errors of fatty acid oxidation, dicarboxylates accumulate in plasma and are excreted in urine (113). Wada & Usami (125) hypothesized that, in normal subjects, dicarboxylates can be β-oxidized directly to succinate, without passing by acetyl-coenzymeA (CoA) and the citric acid cycle (CAC). This would provide a mechanism for conversion of carbon from even-chain fatty acids to glucose. To test this hypothesis, Tserng & Jin (122) incubated rat liver homogenates with [1,2,3,4-$^{13}C_4$]dodecanedioate. Succinate isolated from the medium was enriched in M4, demonstrating the gluconeogenic potential of dodecanedioate. M2 succinate, also detected, derived presumably from the metabolism of [1,2-$^{13}C_2$]acetyl-CoA in the CAC. In control experiments with the monocarboxylate [1,2,3,4-$^{13}C_4$]dodecanoate, succinate was only enriched in M2. The in vivo contributions of fatty acid ω-oxidation to fatty acid catabolism and to gluconeogenesis remain to be determined.

Probing the Origin of the Two N Atoms of Urea

Brosnan et al (13) perfused rat livers with $^{15}NH_4Cl$ of various enrichments and assayed the MID of urea, glutamine, citrulline, and aspartate, as well as the positional isotopomer distribution of glutamine. They demonstrated (Figure 2) that the relative proportions of the urea isotopomers depend on the relative and absolute enrichments of ^{15}N in the two precursor pools of urea nitrogen (mitochondrial ammonia and cytosolic aspartate). Also, they showed that the ^{15}N enrichment of citrulline and aspartate in the effluent perfusate can be used as proxies for those of mitochondrial ammonia and cytosolic aspartate.

Investigation of Transamination in Synaptosomes

To study glutamine metabolism in brain cells via glutaminase and transaminase reactions, Yudkoff et al (133) incubated rat brain synaptosomes with [2,3,3,4,4-$^2H_5$]glutamine (M5). Within 5 min of tracer addition, glutamate became enriched in M5 and M4 isotopomers. M5 glutamate is formed directly from the glutamine tracer through the action of glutaminase. It is converted to M4 glutamate through the following sequence of reactions catalyzed by aspartate aminotransferase: [2,3,3,4,4-$^2H_5$]glutamate (M5) + oxaloacetate $\rightarrow$ [3,3,4,4-$^2H_4$]αKG (M4) + aspartate; and [3,3,4,4-$^2H_4$]αKG (M4) + aspartate $\rightarrow$ [3,3,4,4-$^2H_4$]glutamate (M4) + oxaloacetate. The similar glutamate enrichments in M5 and M4 glutamate shows that the reversible aspartate aminotransferase reaction is severalfold faster than the flux through the CAC.

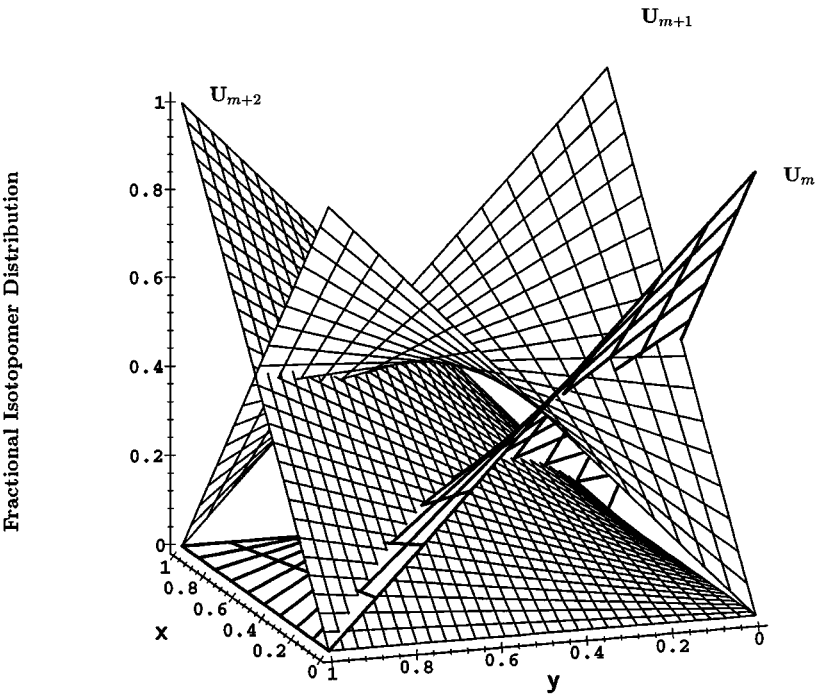

Figure 2 Theoretical relative abundance of the nitrogen mass isotopomers of urea. These are plotted as a function of the fractional abundance of ^{15}N in the mitochondrial ammonia pool (x) and the cytoplasmic aspartate pool (y). U_m U_{m+1}, and U_{m+2} are, respectively, the isotopomers of urea that contain zero, one, and two atoms of ^{15}N. Reproduced from Reference 13 with permission.

Ketone Body Metabolism

Measurements of ketone body turnover in vivo require separate tracing of R-β-hydroxybutyrate (R-BHB) and acetoacetate (AcAc). This is conveniently achieved by infusing a mixture of [3,4-$^{13}C_2$]AcAc (which equilibrates with R-[3,4-$^{13}C_2$]BHB) and of R-[1,2,3,4-$^{13}C_4$]BHB (which equilibrates with [1,2,3,4-$^{13}C_4$]AcAc. The M2 and M4 enrichments of plasma R-BHB and AcAc are monitored and computed in models developed by Cobelli et al (4, 21).

Three processes contribute to the isotopic dilution of plasma ketone bodies. First, net ketogenesis occurs in liver via the mitochondrial HMG-CoA cycle. Second, an isotopic exchange or pseudoketogenesis, originally hypothesized by Landau (72), occurs in peripheral tissues via the reversal of 3-oxoacid-CoA transferase. This process exchanges labeled plasma AcAc for the unlabeled acetoacetyl moiety of AcAc-CoA derived from fatty acid β-oxidation without

net ketogenesis (31). Third, partial scrambling of the label between the two acetyl moieties of plasma AcAc occurs in peripheral tissues via the combined reversals of AcAc-CoA thiolase and 3-oxoacid-CoA transferase (31, 41). This forms [1,2-$^{13}C_2$]AcAc from [3,4-$^{13}C_2$]AcAc. This scrambling can be monitored by GC-MS, since the spectra of AcAc and R-BHB include ions corresponding to C1-C4 and C3-C4 of each species.

Pseudoketogenesis and scrambling of AcAc label were identified by administering [3,4-$^{13}C_2$]AcAc to hepatectomized dogs, a preparation in which no net ketogenesis takes place (31). In these experiments, [1,2-$^{13}C_2$]AcAc and [1,2,3,4-$^{13}C_4$]AcAc accumulated. These exchanges are stimulated by dichloroacetate, a pyruvate dehydrogenase activator (26), which lowers the rate of ketone body uptake. Scrambling of AcAc label is obvious after bolus injection of labeled AcAc (31), but it is technically difficult to detect (31), or goes undetected (3), during constant infusion of the tracer. The nondetection of the label-scrambling epiphenomenon does not exclude pseudoketogenesis.

Pseudoketogenesis may explain why some reported rates of ketone body turnover in diabetic ketoacidosis far exceed basal metabolic rates (40). Since ketogenesis and pseudoketogenesis cannot be differentiated by isotopic dilution, new protocols must be developed to assess the rate of net ketogenesis in humans.

Glycerol Production and Cycling in Liver

The classical concept of glycerol metabolism involves production via lipolysis in peripheral tissues (mostly adipose tissue) and hepatic utilization via glycerol kinase (25). Recent studies by Previs et al (110) showed that rat liver releases glycerol by hydrolysis of glycerides and by an α-glycerophosphate $\rightleftharpoons$ triose phosphate cycle. Isolated rat livers perfused in open circuit with [U-$^{13}C_3$]glycerol released unlabeled glycerol, presumably via the action of hepatic lipases on tissue triacylglycerols. Also, when dogs were infused with [$^2H_5$]glycerol, the glycerol enrichment in the hepatic vein was lower than that of the weighted average of the portal vein and hepatic artery enrichments (111).

When rat livers were perfused with 0.1–3.5 mM [$^2H_5$]glycerol (110), M1 to M4 glycerol isotopomers were released (Figure 3). This suggested the operation of a substrate cycle between extracellular glycerol and liver triose phophates, where ^2H is lost in the reversible reactions catalyzed by α-glycerophosphate dehydrogenase, triose phosphate isomerase, and glycolytic enzymes. The formation of M4, M3, and M2 glycerol isotopomers is explained by cycling between [$^2H_5$]glycerol and (*a*) dihydroxyacetone phosphate, (*b*) glyceraldehyde 3-phosphate, and (*c*) glycolytic intermediates between glyceraldehyde 3-phosphate and phosphoenolpyruvate (PEP), respectively. Additional cycling through the PEP-pyruvate-oxaloacetate-PEP cycle forms M1 and probably

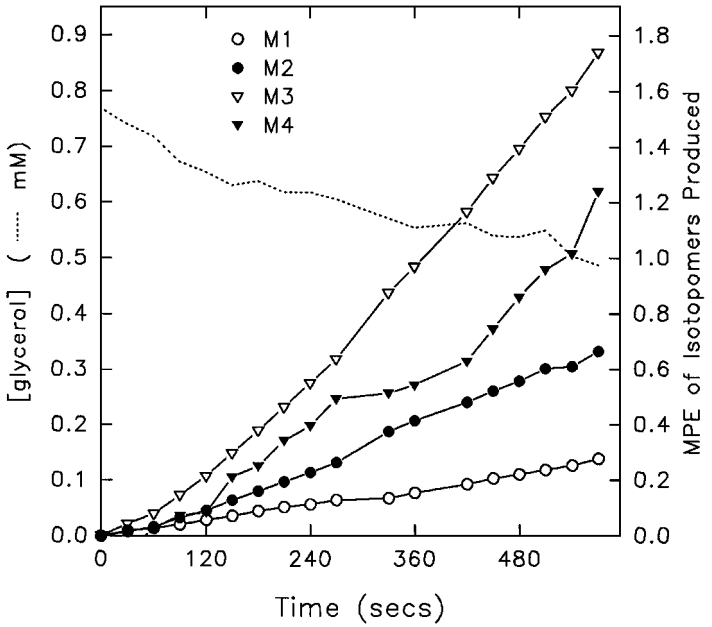

Figure 3 Loss of ^2H from [$^2H_5$]glycerol in the perfused rat liver. A liver was perfused with 300 ml of recirculating perfusate containing [$^2H_5$]glycerol at an initial concentration of 0.8 mM. The decrease in total glycerol concentration is shown by the broken line. Perfusate glycerol was progressively enriched with M1–M4 mass isotopomers identified in the caption. MPE, Mole percent enrichment. Reproduced from Reference 110 with permission.

unlabeled glycerol. In all cases, the cycling process must involve α-glycerophosphate hydrolysis, which probably occurs through phosphatases, since the glycerol kinase reaction is irreversible. The rate of release of M1 to M4 glycerol isotopomers corresponded to 7–10% of the rate of uptake of M5 glycerol. The impact of this cycle on measurements of glycerol turnover is minimal in vivo, at least in the dog, since identical rates of glycerol turnover were measured with an infused mixture of [2-^{13}C]glycerol and [$^2H_5$]glycerol (111).

Absorption and Metabolism of Amino Acids

Some amino acids that are nonessential in healthy adults become essential under special conditions, such as fasting, pregnancy, infant growth, trauma, and immunological stress. To estimate whole-body and splanchnic metabolism of dietary amino acids, elegant protocols were developed that involve the simultaneous administration of different mass isotopomers of one or more amino acids by the intravenous and intragastric routes (10, 17, 98, 123). Rates of amino acid

synthesis are calculated from the extent to which the ^{13}C, ^{2}H, or ^{15}N in the amino acid tracer is diluted in excess of the dilution that would have been expected from the entry of that amino acid from the diet and from tissue proteolysis.

In other studies, pathways of synthesis of some amino acids were explored by administration of uniformly ^{13}C-labeled amino acids, either singly or as labeled proteins extracted from *Spirulina platensis* algae grown under 99% labeled $^{13}CO_2$. The labeled algae were incorporated into the diet of animals and humans (6, 7), and amino acids were isolated from plasma or from proteins. The MID of these amino acids showed (*a*) the original fully labeled isotopomers, reflecting direct incorporation of the dietary amino acids into proteins and/or (*b*) lower mass isotopomers, reflecting synthesis from various labeled products derived from the algae. Although in most cases, rates of synthesis cannot be calculated because the enrichment of the precursors is unknown, the observed MID patterns can be interpreted in light of current concepts of amino acid essentiality/nonessentiality. For example, in a study conducted in fed and fasted women (7), plasma proline was enriched only in M5 in the fed state. However, in the fasted state, it became enriched in all mass isotopomers except M3, reflecting some de novo synthesis. It was concluded that proline synthesis is either strictly regulated by dietary proline or is substantially compartmentalized.

Intestinal Absorption and Metabolism of Purines and Pyrimidines

The production of purines and pyrimidine nucleotides, precursors of nucleic acids, proceeds by de novo synthesis and by the so-called salvage pathways of preformed bases or nucleosides (derived from nucleic acid catabolism and from the diet). The absorption and metabolism of dietary nucleic acids have been investigated by using *Spirulina platensis* algae grown under 99% enriched $^{13}CO_2$. Berthold et al (5) fed hens and mice with whole labeled algae, while Boza et al (11) fed mice with U-^{13}C-labeled nucleotides or amino acids isolated from the algal biomass. Variables in the mice studies included pregnancy and diet (normal vs nucleic acid–deficient). Nucleic acids, isolated from liver, intestinal mucosa, or whole fetuses, were hydrolyzed to nucleosides that were subjected to MID analysis. The presence of M8, M9, and M10 nucleosides reflects the direct incorporation of dietary purine and pyrimidine nucleosides. M5 nucleosides are formed by the incorporation of either ribose or purine base. M4 nucleosides are formed by the incorporation of a pyrimidine base. M3 nucleosides are formed by the incorporation of [U-$^{13}C_4$]aspartate, which contributes three carbons to the pyrimidine ring. M2 nucleosides result from the incorporation of [1,2-$^{13}C_2$]glycine. Last, M1 nucleosides can derive from the independent incorporation of single-carbon presursors (bicarbonate and methenylhydrofolate).

As a whole, the MID data indicated (*a*) that a large majority of bases incorporated into maternal and fetal murine ribonucleic acids derives from de novo synthesis and (*b*) that some dietary uracil and uridine are incorporated into nucleic acids. These findings are in keeping with the immunological benefit resulting from the inclusion of either nucleic acids or uracil alone in the diet. They suggest that pyrimidines are conditionally essential nutrients (16).

Reversibility of the Isocitrate Dehydrogenase Reaction

In the CAC, the conversion of isocitrate (ICIT) to α-ketoglutarate (αKG) is catalyzed by two isocitrate dehydrogenases (ICDH), which are NAD^+- and $NADP^+$-dependent, respectively. On the basis of in vitro studies, Sazanov & Jackson (116) proposed that in the mitochondrial matrix, a substrate cycle operates between ICIT and αKG, where NAD^+-ICDH generates αKG, and $NADP^+$-ICDH regenerates ICIT. The ICIT $\rightleftharpoons$ αKG cycle would provide a mechanism by which the flux through the CAC is tightly controlled by the modifiers of NAD^+-ICDH and by the energy state of the inner mitochondrial membrane. To test this hypothesis in an intact tissue, Des Rosiers et al (28) perfused isolated rat livers with [U-$^{13}C_5$]glutamate and measured the MID of CAC intermediates. The M5 enrichments of αKG and citrate were 24% and 11%, respectively. The M4 enrichments of succinate, fumarate, and malate were 16, 3, and 3%, respectively. The M3 enrichment of pyruvate was only 1.3%.

Similar data were observed with [U-$^{13}C_5$]glutamine. Under these conditions, M5 citrate can only be formed by carboxylation of M5 αKG via the reversal of the aconitase and ICDH reactions. An alternate mechanism is through the condensation of M2 acetyl-CoA and M3 OAA, formed through the metabolism of M5 αKG into the CAC and into pyruvate. This can be excluded because of the low enrichments in M4 malate, M3 pyruvate, and M1 to M4 citrate. From the enrichment ratio (M5 citrate)/(M5 αKG), one calculates that 45% of citrate molecules are formed via the reversal of the ICDH reaction. In the rat heart perfused with [U-$^{13}C_5$]glutamate the reversal of the ICDH reaction amounts to 5% and 16% of the CAC rate, in normoxia and low-flow ischemia, respectively (23; B Comte & C Des Rosiers, unpublished data). The interconversion between isocitrate and αKG, observed in intact organs, is consistent with Sazanov and Jackson's hypothesis (116).

Succinate Formation in the Heart by the Oxidative and Reductive Pathways

In the oxygen-deprived heart, the protective effects of fumarate have been linked to its conversion to succinate through oxidative and reductive pathways. Fumarate oxidation to succinate occurs through normal operation of the CAC,

while its reduction to succinate is catalyzed by the reversal of the succinate dehydrogenase (or fumarate reductase) reaction. Both pathways are linked to substrate-level phosphorylation reactions (53). However, there is disagreement about the relative contributions of these two pathways. To clarify this question, Laplante et al (78) perfused rat hearts with 11 mM glucose, 1 mM lactate, 0.2 mM pyruvate, 0.4 mM [U-$^{13}C_4$]fumarate, and 0.2 mM unlabeled or [1-^{13}C]octanoate, and then measured the MID of tissue and effluent CAC intermediates.

In the presence of unlabeled octanoate, and under all conditions tested (normoxia, low-flow ischemia, or hypoxia), tissue and effluent succinate were labeled on all four carbons (up to 15% enrichment). M4 succinate could be formed only through the reversal of the succinate dehydrogenase reaction. The alternate mechanism would require the formation of M6 citrate, the enrichment of which was negligible. M2 and M1 succinate were not detected, indicating negligible conversion of exogenous fumarate to succinate by the oxidative pathway. However, the CAC was fueled by substrates other than exogenous fumarate—mostly by octanoate. This conclusion was based on the appearance of M1 succinate in perfusions with both [1-^{13}C]octanoate and [U-$^{13}C_4$]fumarate. As a whole, the MID data show an increase in the reductive pathway during oxygen deprivation, supporting a role of this pathway in the cardioprotective effect of fumarate.

Glucose Metabolism and Recycling

Isotopic investigations of glucose metabolism in vivo are complicated by intra- and interorgan substrate cycles and by numerous isotopic exchange reactions (reviewed in 60 and 71). A number of authors (8, 20, 57–59, 61–63, 65, 69, 77, 87, 90, 130) have used [U-$^{13}C_6$]glucose and MID analysis for in vivo and in vitro investigations of glucose turnover, glycolysis, GNG, glycogenesis, Cori cycling, pyruvate cycling, and the CAC. Let us briefly review the fates of [U-$^{13}C_6$]glucose.

Through glycolysis, M6 glucose forms M3 pyruvate, which equilibrates with lactate and alanine (58, 64, 130). Reactions of the pyruvate cycle and the CAC convert M3 pyruvate to M1 and M2 pyruvate, as well as M1 to M3 PEP. Condensation of two triose phosphates can yield M1 to M6 isotopomers of free glucose and glycosyl units of glycogen. However, a low enrichment of the infused tracer [U-$^{13}C_6$]glucose minimizes the formation of M4 to M6 glucose units. Thus plasma M6 glucose arises only from the infused tracer, and the M6 enrichment of plasma glucose can be used to measure glucose turnover without interference of recycled tracer. M1 to M3 glucose reflect recycling of label from [U-$^{13}C_6$]glucose through the Cori cycle, which shares reactions with GNG.

The contribution of recycling to glucose production was investigated first by using mass fragmentography analysis (reviewed in 60), then by using MID analysis (20, 58, 59, 63, 69, 81). In normal humans and rats, the glucose recycling range was 6–37% of hepatic glucose output. These values were calculated from the MID data using mathematical models of variable complexity (20, 57–59, 63, 69, 81).

Compared to normal subjects, the accumulation of M1 to M3 glucose in plasma was increased in children deficient in glycogen debranching enzyme (type III glycogen storage disease), but it was negligible in children deficient in glucose-6-phosphatase (type I) (58, 59). Infusion of [U-$^{13}C_6$]glucose can thus be used to differentiate these diseases without performing a liver biopsy.

Synthesis of Liver Glycogen by the Direct and Indirect Pathways

After liver glycogen depletion caused by fasting, ingestion of a carbohydrate meal leads to glycogen repletion by two mechanisms. In the direct pathway, dietary glucose is incorporated as intact C_6 units into glycogen. In the indirect pathway, glucose is first split into C_3 units in peripheral tissues and possibly in pericentral hepatocytes. Then, C_3 units are converted to glycosyl units in liver using reactions of GNG. When the carbohydrate meal is enriched with [U-$^{13}C_6$]glucose, MID analysis of glucose isolated from liver glycogen allows calculation of the contribution of the two pathways of glycogen repletion (20, 29, 57, 62, 63, 65). M6 enrichment derives from the direct pathway, while M1 to M3 enrichment derive from the indirect pathway. In normal rats the contribution of the direct pathway is 34–71%. As above, these percentages were calculated with varying mathematical expressions, based on somewhat different assumptions (20, 29, 57, 62, 63, 65).

Studies of hepatic glycogen repletion in humans can be conducted noninvasively using the acetaminophen glucuronide probe (35, 46, 47, 93). After administration of the tracer, acetaminophen is ingested or infused. The drug is conjugated in liver with glucuronate, the labeling pattern of which is close to that of glycosyl units incorporated into glycogen. The glucuronide is isolated from urine, and the MID of its glucuronate moiety is assayed by GC-MS (46, 73, 115). Note that acetaminophen glucuronidation is not uniform across the human liver lobule. It appears to predominate in perivenous hepatocytes (35), while GNG and glycogen synthesis predominate in periportal hepatocytes (56). Thus caution must be exercised when interpreting data gathered with the acetaminophen probe. However, in the rat, the relative contributions of the direct and indirect pathways, assessed by MID analysis, appeared equal in periportal and perivenous areas of the liver lobule (20).

Citric Acid Cycle Parameters

During the past decade, studies of the interrelation of the CAC and other pathways have benefited greatly from the use of uniformly ^{13}C-labeled substrates and MID analysis. These complemented and extended the scope of studies conducted with singly labeled ^{13}C and ^{14}C tracers that used mass fragmentography, nuclear magnetic resonance (NMR), or chemical degradation techniques (9, 18, 22, 32, 60, 89, 94–96, 99, 118, 124, 127). MID analysis allowed new inroads in determinations of (*a*) the flux ratios (pyruvate carboxylase)/CAC, (pyruvate carboxylase)/(pyruvate dehydrogenase), (pyruvate kinase)/(pyruvate carboxylase), (*b*) the degree of isotopic randomization in the malate dehydrogenase and fumarase reactions, and (*c*) the extent of dilution of gluconeogenic tracers by isotopic exchanges with the CAC (27, 38, 63, 64, 80, 81, 87).

In perfused livers or hepatocyte incubations, by using [U-$^{13}C_3$]lactate and/or [U-$^{13}C_3$]pyruvate as tracer, the ratio pyruvate kinase (PK)/pyruvate carboxylase (PC) is obtained directly from the enrichment ratio M2/M3 of tissue pyruvate or alanine (27). Similarly, in rat hearts perfused with these tracers, the PC/pyruvate dehydrogenase (PDH) ratio is obtained from the enrichment ratio [M3 of C-1+2+3+6]/[M2 C-4+5] of tissue of effluent citrate. Since citrate is a chemically symmetrical molecule it needs to be cleaved enzymatically to its acetyl and oxaloacetate (OAA) moieties (23, 24).

The calculation of the other CAC parameters mentioned above require measuring the MID of plasma or liver glucose (63, 64, 80, 81, 87). One could also measure the MID of other GNG or CAC intermediates or related metabolites (e.g. αKG, glutamate, glutamine, PEP) isolated from plasma, effluent perfusate, or tissue (27, 38, 64, 80). In monkeys infused with [U-$^{13}C_3$]lactate, the MID of plasma glutamate (not glutamine) reflected that of liver αKG (132). In monkeys given phenylacetate, the MID of liver αKG is reflected by that of the glutamine moiety of phenylacetylglutamine isolated from urine (132). This noninvasive probing of liver CAC intermediates had been introduced by Magnusson et al (94, 118). Phenylacetylglutamine is formed in liver from the conjugation of glutamine and phenylacetate (exogenous or derived from phenylalanine catabolism). Some amino acids (alanine, serine, glutamate) derived from very low density lipoprotein (VLDL)-apolipoprotein B-100 can also be used as noninvasive probes of the labeling of hepatic CAC and GNG intermediates (8, 130).

Calculation of the CAC parameters from the MID of the measured metabolites requires either solving Lee's quadratic equation (81) or a more complex mathematical treatment (27, 38, 80). The simple quadratic equation yields the dilution factor for correcting rates of GNG, glucose recycling, and the contribution of the indirect pathway for glycogen synthesis (20, 63, 69, 87).

However, when using the quadratic equation, one of the assumptions is that pyruvate dehydrogenase and/or pyruvate kinase activities are negligible. Although pyruvate dehydrogenase activity can be neglected in fasting, it is increased up to 10-fold by glucose administration (94). Thus in studies where substrate amounts of [U-$^{13}C_6$]glucose are administered to fasted subjects or animals (8, 20, 63, 69, 87), the PC/CAC ratio and the extent of label randomization in OAA are probably underestimated.

In contrast, the dilution factor and, thus, the corrected rates of GNG are overestimated up to twofold. This degree of overestimation was calculated by comparing values of these parameters calculated using the quadratic equation (87) and later models that include PDH and PK activities (27, 80). Other processes to be considered in these calculations are exchange reactions between CAC intermediates and amino acids, $^{13}CO_2$ reincorporation, and reversibility of ICDH reaction (for more details see 27, 39, 64, 80). Since these processes result in different, sometimes opposing, variations in the value of the calculated CAC parameters, their overall effect is difficult to assess.

Involvement of ATP-Citrate Lyase in Gluconeogenesis from Lactate

GNG from lactate or pyruvate involves mitochondrial carboxylation of pyruvate to OAA. The mechanism by which the carbon skeleton of OAA is transferred to the cytosol, before PEP formation, depends on whether reducing equivalents need to be transported to the cytosol for the glyceraldehyde-3-phosphate dehydrogenase reaction. During GNG from pyruvate or lactate, the skeleton of OAA is transferred as malate or as aspartate, respectively.

Des Rosiers et al (27) perfused rat livers with [U-$^{13}C_3$]lactate plus [U-$^{13}C_3$]pyruvate and measured the MID of a dozen intermediates of the CAC and of GNG. The data were introduced into mathematical models of increasing complexity (38). Some of the models hinted at heterogeneity of metabolite labeling because the MID of sequential intermediates were incompatible. The best fit of data, with no indication of labeling heterogeneity, was obtained by using a model that included (*a*) the reversal of the ICDH reaction, and (*b*) the transfer to the cytosol of the carbon skeleton of OAA derived from lactate *via* ATP-citrate lyase. In other livers perfused with [U-$^{13}C_5$]glutamate or [U-$^{13}C_5$]glutamine (28 and see above), the detection of M5 citrate and M3 malate provided additional support for the occurrence of these reactions in fasted rat livers.

ATP-citrate lyase, the activity of which is induced by carbohydrate feeding, accounts for most of the transfer of lipogenic acetyl-CoA from mitochondria to cytosol by the citrate cleavage pathway (14, 36). However, in rats, after two days of fasting, the ATP-citrate lyase activity of the liver is still one half that

of fed rats (27). This remaining activity is sufficient to account for the rate of GNG from lactate. The contribution of the citrate cleavage pathway to GNG at various stages of fasting remains to be investigated.

Caveat: Secondary Tracers

The long-term in vivo infusion of a multiply labeled substrate often results in the formation of lower-mass isotopomer(s) of the infused substrate. For example, M2 and M1 lactate appear during infusion of [U-$^{13}C_3$]lactate, and M1 to M3 glucose appear during infusion of [U-$^{13}C_6$]glucose (20, 63, 64, 69, 81, 87). In addition, other plasma substrates become labeled. For example, lactate and bicarbonate become labeled during infusion of [1,2-$^{13}C_2$]acetate or [U-$^{13}C_6$]glucose (121). As discussed earlier, the appearance of these labeled products yields information on the metabolism of the infused substrate. For example, the production of M2 and M1 lactate from [U-$^{13}C_3$]lactate (132) results from the operation of the cycle: pyruvate → OAA → PEP → pyruvate. This cycle is linked to randomization of OAA labeling via malate dehydrogenase and fumarase and to partial exchange of OAA carboxyl label with unlabeled CO_2. Note that these newly labeled substrates become secondary tracers that are also metabolized to products, the labeling pattern of which may differ from that resulting from the metabolism of the infused tracer. This may complicate the interpretation of data from long-term tracer experiments.

During infusion of [U-$^{13}C_6$]glucose, the production of M1 to M3 glucose may affect the calculation of the contribution of the direct pathway of liver glycogen synthesis (29). Also, during the infusion of [2-^{13}C]acetate, labeled CO_2 and glutamine released by muscle into the blood affect the labeling pattern of liver CAC intermediates and of glucose. This is why the labeling pattern of glutamate, extracted from an isolated rat liver perfused with [2-^{13}C]acetate, is different from that of glutamate extracted from the liver of a rat infused with [2-^{13}C]acetate (9). The labeling patterns of glucose are also different in the two types of experiments.

USE OF MID TO MEASURE THE RATE OF SYNTHESIS OF POLYMERIC MOLECULES

Principles, History, and Conditions of Validity

A well-recognized limitation in the study of the biosynthesis of molecules using isotopes has been the difficulty in using the amount of isotope incorporated into a product to calculate the rate of synthesis. Since labeled substrates traversing metabolic pathways are diluted in specific activity or enrichment, the incorporation of label into the product underestimates the total incorporation of precursor. It is often not possible to determine the actual enrichment of the precursor, thus

the correct rate of synthesis cannot be calculated. We outline below the historical development of important new methods that circumvented this limitation and have expanded new avenues for the quantitative analysis of metabolic flux.

In 1985, Strong et al (120) described a method for quantifying the isotopic enrichment of a product formed by a specific biosynthetic pathway. Their method is applicable to biosyntheses incorporating mass isotopes into specific products detected by GC-MS. It requires that more than one labeled precursor atom be incorporated into the product of interest. They used as an example the biosynthesis of uracil, which contains two N atoms, from ^{15}N-labeled precursors. The method does not require that the same pathways be used to label each of the two N atoms, and thus does not assume that the enrichment of each N precursor is identical. However, it requires finding two fragment ions to measure the enrichment of each N atom of uracil. With this information and the MID of an ion containing both N atoms, a simple quadratic equation was used to solve for F, the fraction of pyrimidine molecules synthesized de novo during the labeling period. Then $(1 - F)$ is the portion that was present before the labeling period began or that was produced by an alternative pathway not involving the incorporation of ^{15}N. The key to the calculation is the frequency of occurrence of ^{15}N at both N positions in uracil. Without it, F cannot be determined.

The method described by Strong et al was dependent on mass spectrometry to visualize the incorporation of label and was not directly applicable to NMR experiments. However, Malloy and coworkers independently developed an NMR method for determining the enrichment of heart mitochondrial acetyl-CoA (95, 96). When the CAC is fueled by a ^{13}C-labeled substrate that labels C2 of acetyl-CoA, C_4 of glutamate becomes labeled. The labeling of glutamate C_4 alone provides no information about the rate of the CAC because of the unknown dilution of the tracer. However, on the next turn of the cycle, some label appears in C2 of OAA. When this isotopomer combines with [2-^{13}C]acetyl-CoA to form citrate, C_3 and C_4 of glutamate are both labeled. These adjoining ^{13}C atoms are visible in proton-decoupled ^{13}C NMR as a doublet. The probability of observing a ^{13}C-^{13}C versus ^{12}C-^{13}C quantifies the enrichment of the acetyl-CoA pool feeding the CAC. These researchers have also shown that the enrichment of acetyl-CoA can be obtained from the multiplet labeling patterns of succinate carbons. In both methods, the key information is the incorporation of a second labeled acetyl unit into a metabolite.

The first application of MID to the synthesis of a polymer, i.e. palmitate, was presented by Hellerstein et al (45), who coined the acronym MIDA (mass isotopomer distribution analysis). They reasoned that the MID of palmitate synthesized from labeled acetate could be used to calculate the enrichment of lipogenic acetyl-CoA. They computed the excess signal (over baseline) at various masses (45, 48) to calculate the precursor enrichment, *p*. Then, the

fraction of total lipid resulting from de novo lipogenesis was calculated from the per-carbon enrichment (49). Hellerstein and colleagues used MIDA in many investigations on the syntheses of fatty acids, cholesterol, glucose, and proteins.

Kelleher and colleagues (67, 68, 70) used a different technique, i.e. isotopomer spectral analysis (ISA), for in vitro biosynthesis where precursor are used at much higher enrichments than in vivo. Thus at least 13 isotopomers of palmitate were detected. They used nonlinear regression to calculate the precursor dilution parameter, *D*, and the fraction of newly synthesized product g(*t*). More recently, the natural abundance at each mass has been included in the regression routine (70). ISA provides (*a*) statistical estimates of the error in the fit of model to data, and (*b*) covariance analysis that yields insight into parameter interdependence.

Contributions to the theoretical basis of these techniques have also been presented by Lee and coworkers (84–86). They demonstrated the principles of MIDA elegantly with the test tube synthesis of an artificial polymer, glucose pentaacetate made from increasingly enriched [^{13}C]acetic anhydride. Although each of the above methods was developed independently, they can be seen retrospectively to share common ground in the theory underlying each approach. Chinkes et al (19) have compared the mass isotopomer dilution methods that have been published to compute production of VLDL fatty acids in humans. The various computations yield comparable rates, overall, especially when MID data are measured carefully.

The validity of the MIDA and ISA techniques requires that all monomeric units associating to form the newly synthesized polymeric molecules have the same enrichment. Variations in the enrichment of the labeled precursor over time or in different spatial compartments lead to errors. To illustrate these conditions, consider a couple of simple theoretical examples (Figures 4 and 5). Glucose can be considered as a dimer made of two identical C_3 units, the triose phosphates. In Figure 4, the continuous lines are the theoretical distributions (Equation 3) of M, M1, and M2 glucose synthesized from a homogeneous pool of triose phosphates increasingly labeled from [2-^{13}C]glycerol. The vertically aligned solid symbols represent the MID of glucose made from 60% enriched triose phosphates. If this newly synthesized labeled glucose is mixed with an equal amount of unlabeled glucose (derived from glycogenolysis), the MID of the mixture is represented by the open symbols, which are no longer vertically aligned. The arrows show the shifts in the proportions of individual isotopomers resulting from the dilution. The enrichment of the triose phosphates and the extend of dilution of newly synthesized glucose by unlabeled glucose can easily be calculated.

Consider now the mixing of two equal amounts of glucose made from two pools of triose phosphates of different enrichments (20% and 5%) (Figure 5).

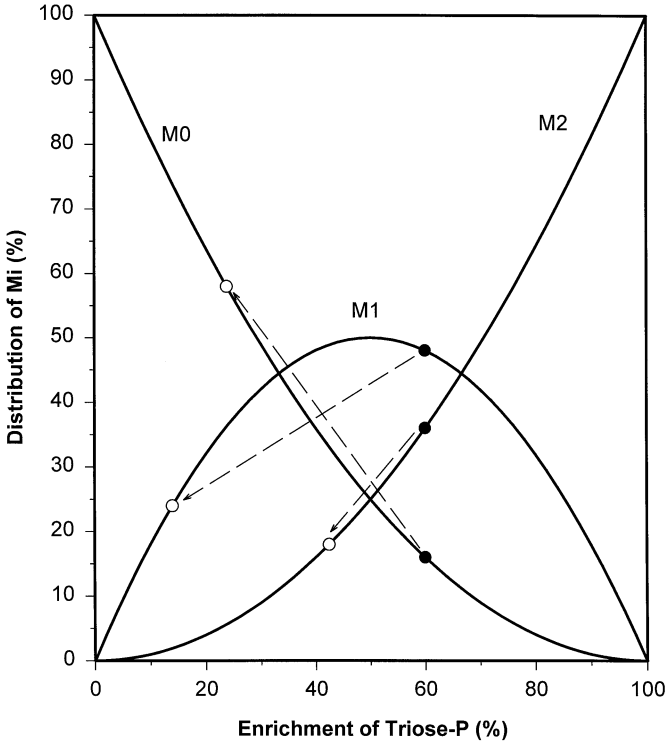

Figure 4 Influence of preformed unlabeled glucose on the MID of labeled glucose synthesized from [2-^{13}C]glycerol. The continuous lines are the theoretical distributions of M, M1, and M2 isotopomers calculated from Equation 3. The solid symbols represent the MID of glucose made from a single homogeneous pool of 60% enriched triose phosphates. When this newly synthesized labeled glucose is mixed with an equal amount of unlabeled glucose, the MID of the mixture is represented by the open symbols, which are no longer vertically aligned. The arrows show the shift in the proportion of each isotopomer resulting from the dilution. Mi, percentage of each isotopomer; triose-P, triose phosphate.

Neither pool of newly made glucose is diluted with unlabeled glucose (f = 100% for each pool). Computation of the MID of the mixture yields erroneous values for the enrichment of the triose phosphates and for the extent of dilution (Figure 5, *bottom*). Note that the calculated values are not the averages of the actual parameters of the two pools. This is because the precursor enrichment appears in the equations for the amount of each isotopomer as a nonlinear parameter. Similar calculations have been applied to the mixing of multiple pools of labeled glucose (110) and to variations in the acetyl-CoA enrichment

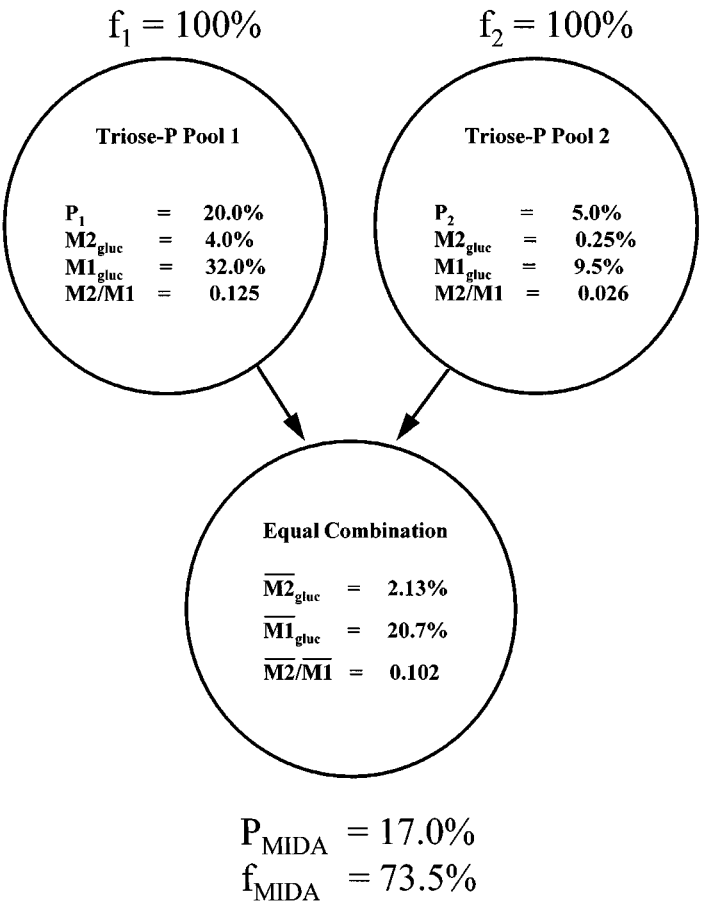

Figure 5 Combination of two pools of glucose of equal size made from triose phosphates labeled from [2-^{13}C]glycerol with an M1 MPE (P) of 20% (Pool 1) and 5% (Pool 2). Each primary pool is constrained with an *f* of 100% (no dilution by unlabeled glucose). The combined pool (which would be measured in liver effluent) has a mass isotopomer distribution (MID) of glucose from which an artifactual *f* of 73.5% is calculated. Triose-P, triose phosphate. Reproduced with modifications from Reference 110 with permission.

(66). We now consider various applications of MID to study the synthesis of complex molecules.

De Novo Synthesis of Pyrimidine in Hepatocytes

The two N atoms of the uracil molecule derive from carbamyl-phosphate and aspartate. In hepatocytes, these two substrates can be labeled from either $^{15}NH_4Cl$

or L-[5-^{15}N]glutamine. Strong et al (120) determined the mass and positional isotopomer distribution of uracil isolated from hepatocytes incubated with the above substrates. In the presence of $^{15}NH_4Cl$, the two N atoms were equally labeled. From the MID of uracil (M, M1, M2), Strong et al calculated the enrichments of carbamyl-phosphate and aspartate and the fraction of uracil neosynthesis. In the presence of L-[5-^{15}N]glutamine, the two N atoms of uracil were unequally labeled, as determined by mass fragmentography. Introducing the enrichments of each N in their equations, Strong et al calculated the enrichments of the precursors and the fraction of neosynthesis. This fraction was stable with $^{15}NH_4Cl$ but increased progressively with L-[5-^{15}N]glutamine.

Fatty Acid Synthesis

Studies of fatty acid synthesis using deuterated water represent an early application of MID analysis. In 1937, Shoenheimer & Rittenberg (117) reported that enrichment of body water with ^{2}H (by ingestion of ^2H_2O) led to incorporation of ^{2}H in fatty acids. In lipogenic organs synthesizing fatty acids from glucose, protons from water are incorporated in C-H bonds of fatty acids via glycolysis, cytosolic cleavage of citrate (92) and acetoacetyl-CoA (36), and reduction reactions involving NADPH plus H^+. NADPH becomes labeled in reactions of the pentose pathway, ICDH, and malic enzyme (92). Since some ^{2}H is incorporated before the cytosolic acetyl-CoA stage, the ^{2}H/C incorporation ratio varies somewhat with the carbon source (36, 37).

The first quantitative analysis of proton incorporation into fatty acids was reported by Jungas (55), who incubated rat adipose tissue in buffer made with 100% ^2H_2O and containing glucose. GC-MS analysis of tissue palmitate (as methyl ester) revealed the presence of a cluster of newly synthesized isotopomers containing 14–28 ^{2}H atoms, with an average of 22. This represents the statistical distribution of the number of protons from water incorporated in the reactions between glucose and palmitate. This value could not be calculated theoretically because the magnitude of the isotope effects and isotopic exchanges in the numerous reactions cannot be calculated.

Wadke et al (126) reported similar palmitate labeling in rat livers perfused with 100% ^2H_2O buffer. Also, a dual pattern of stearate labeling was observed: A large cluster at M17–M31 centered on M24, and a small cluster centered at M1-M4. The latter cluster was identified by increases in the natural enrichments of methyl stearate at these masses. This indicated the simultaneous production of stearate by de novo synthesis and by elongation of preexisting palmitate. When fatty acid synthesis is investigated in vivo, body water is ^{2}H enriched by only a few percent in animals and by a few tenths of a percent in humans. GC-MS analysis of fatty acids reveals only small increases in the proportion of M1 and M2 isotopomers. Lee et al (2, 79, 82, 83) presented equations

to calculate from the MID data the number of deuterium atoms incorporated in fatty acids of different chain length and the fraction of fatty acids that is newly synthesized by total synthesis and by chain elongation. The number of deuterium atoms incorporated has been confirmed by Diraison et al (33, 34).

In 1991 and 1992, Hellerstein et al (44, 45, 48, 49) presented an original technique for investigating fatty acid synthesis in live animals and in humans. After an overnight fast, they infused tracer sodium [1-^{13}C]acetate intravenously for a period of up to 15 h, during which a meal was given. In addition, they administered sulfamethoxazole (SMX), a sulfa drug that is acetylated in liver using extra-mitochondrial acetyl-CoA (48, 52). Plasma samples were collected at different times for isolation of VLDL-triacylglycerols. Transesterification of the latter yielded fatty acid methyl esters, the MID of which was assayed by GC-MS. From the steady-state MID of palmitate, in particular the enrichment ratio M2/M1, Hellerstein et al calculated the fraction of the fatty acids that was synthesized during the experiment and the enrichment of lipogenic acetyl-CoA. In addition, they isolated urinary acetyl-SMX, the enrichment of which (measured by HPLC-MS) was remarkably close to the calculated enrichment of lipogenic acetyl-CoA.

Hellerstein et al (51) are to be credited for the development of (*a*) the MIDA technique for studying the synthesis of fatty acids in liver and (*b*) the noninvasive probe of liver extra-mitochondrial acetyl-CoA with SMX. However, some of the acetyl-SMX data are puzzling—the fact that the labeling of acetyl-SMX was not affected by refeeding, in particular (48, 52). We confirmed their rat experiments (Y Zhang & H Brunengraber, unpublished data), measuring the enrichment of acetyl-SMX by negative chemical ionization GC-MS (135). Since acetyl-SMX is reportedly rapidly cleared by the kidneys (48, 52), the constancy of its enrichment before and after a meal would imply that the increased dilution of the labeling of extra-mitochondrial acetyl-CoA, induced by carbohydrate feeding, is exactly compensated by an increase in [1-^{13}C]acetate uptake.

Other puzzling data on the acetyl probe were gathered by Zhang et al (134), who perfused rat livers with various ^{13}C-labeled precursors of acetyl-CoA and three drugs that are metabolized by acetylation. In most cases, the enrichments of the acetyl-drugs were different. In addition, when drugs were added sequentially to the perfusate, the enrichment of the first acetyl-drug was affected by the presence of the subsequent drugs. It does appears that the liver extra-mitochondrial space contains different N-acetyltransferases, and that the labeling of extra-mitochondrial acetyl-CoA is not homogeneous. Whether this lack of labeling homogeneity affects calculated parameters of fatty acid synthesis remains to be determined.

Hellerstein et al's original technique yields the fraction of the VLDL–fatty acids that is de novo synthesized. In 1993, they presented a method for

determining absolute rates of hepatic fatty acid synthesis (50). They measured (*a*) fractional fatty acid synthesis as above, by infusing [1-^{13}C]acetate; (*b*) the rate of appearance of plasma free fatty acids (FFA), by infusing [1,2,3,4-$^{13}C_4$]palmitate; and (*c*) net fat oxidation by indirect calorimetry. They calculated absolute de novo lipogenesis (DNL) by

$$\text{absolute DNL} = (\text{fractional DNL})[R_a \text{ of FFA} - \text{net body fat oxidation}]. \quad 6.$$

The assumptions of this technique are that all oxidized fat is derived at steady state from circulating FFA and that DNL and FFA reesterification occur exclusively in liver (50). These assumptions are questionable. First, fatty acids are not oxidized in plasma but in tissues, after mixing to an unknown extent with local fatty acids. So, the fractions of the R_a of FFA that are oxidized and reesterified are imprecise. Second, there is good evidence that fatty acid synthesis is not confined to the liver. Third, comparison of R_a of glycerol and FFA measured with tracers and the balance of glycerol and FFA across liver show that the liver cannot be the sole site of FFA reesterification (76). In fairness to Hellerstein et al, they clearly listed the assumptions of their model and considered the possibility that they might be incorrect: "One of our objectives in presenting this method is to stimulate experiments that examine its assumptions" (50).

A puzzling finding of Neese et al (100) was that overfeeding subjects (up to 5500 kcal/day) resulted in minuscule absolute fat synthesis (4–7 g/day, calculated by Equation 6), while the subjects gained 250–500 g/day. The authors assumed that most of the dietary carbohydrate was used to cover the basic metabolic rate, rather than fueling fat synthesis. In fact, it is likely that the bulk of fatty acid synthesis occurred in adipose tissue without being probed by the MIDA technique. This was recently demonstrated by Wolfe et al (1, 1a), who reported that in overfed subjects (4500 kcal/day), rates of whole-body DNL, calculated from indirect calorimetry, were up to 50 times greater than rates of hepatic lipogenesis calculated by MIDA of VLDL-triacylglycerols. They concluded that the liver plays a quantitatively minor role in the conversion of surplus carbohydrate energy into fat and that adipose tissue is probably the main site of fat synthesis.

Cholesterol Synthesis In Vivo

The techniques used to measure fatty acid synthesis in vivo have also been applied to cholesterol synthesis. Incorporation of ^{2}H from ingested ^2H_2O has been used extensively (54, 88). Neese et al (101) infused [1-^{13}C]acetate in humans, measured the the MID of plasma cholesterol, and calculated the fraction of endogenous synthesis. From the decay of labeling of plasma cholesterol over 60 h after the end of label infusion, they calculated rates of absolute cholesterol synthesis, which were similar to rates calculated from fecal sterol balance.

Tracing Lipogenesis with ^{13}C-Labeled Substrates In Vitro

In contrast to in vivo studies in which the enrichment of the lipogenic acetyl-CoA is only a few percent, in vitro studies on cultured cells offer the opportunity to study the MID of fatty acid and cholesterol produced by highly labeled acetyl-CoA. This strategy was exploited by Kelleher and colleagues (67, 68, 70). They incubated cultured cells with various labeled precursors of acetyl-CoA and analyzed the MID of lipids with the ISA technique to calculate various parameters. For example, [^{13}C]acetate supplied to cultured cells at high concentration and enrichment contributed 60–70% of the lipogenic acetyl-CoA pool (67). In 3T3-L1 adipocytes (70) and HepG2 cells (67), [U-$^{13}C_6$]glucose contributed 30% and 80% of lipogenic acetyl-CoA, respectively. These high enrichments of lipogenic acetyl-CoA produce a large number of isotopomers of the product, resulting in an overdetermined model for obtaining the values of the two parameters.

The overdetermined model can be used to probe the assumptions underlying the model. Kharroubi et al (70) used [1,2-$^{13}C_2$]acetate as a precursor for lipogenesis instead of [1-^{13}C]acetate, which is used mostly for in vivo studies. [1-^{13}C]acetate is less expensive per ^{13}C atom, but [1,2-$^{13}C_2$]acetate yields more heavily labeled lipids, thus improving the quality of the parameter estimates. The possible conversion of [1,2-$^{13}C_2$]acetate to singly labeled acetate via the CAC was accounted for by modifying the ISA mode and was found to be very small. The in vitro synthesis of cholesterol from ^{13}C-labeled precursors illustrates an interesting aspect of developing a model for MID. The simplest way to write a model for cholesterol synthesis is as a polymer of acetyl:

$$18 \text{ acetyl} \rightarrow 1 \text{ cholesterol} + 9 \text{ carbons (7 C1 and 2 C2)}.$$

However, labeled or unlabeled carbon can enter cholesterol at the level of acetoacetyl-CoA or mevalonate. Kelleher et al (67) developed a multinomial model for the synthesis of cholesterol that includes all the possibilities for influx in a typical mammalian cell. Thus the synthesis of acetoacetyl-CoA was modeled allowing for influx of labeled or unlabeled four-carbon units as well as the condensation of two-acetyl moieties. The synthesis of HMG-CoA was modeled as a condensation of acetyl unit and acetoacetyl unit. This process was used to build up the C_5 isopentenyl units that condense to form cholesterol. The final model for cholesterol synthesis was

$$4C_5 + C_4 + C_3 \rightarrow 1 \text{ cholesterol}.$$

Thus the investigator may choose between the model of cholesterol as simply a polymer of acetate and this more elaborate model. The latter can be applied when cholesterol synthesis is fueled in part by acetoacetate carbon (36).

Contribution of Gluconeogenesis to Glucose Production

Since glucose can be considered as a dimer made of two C_3 units, the MID of glucose labeled from [2-^{13}C]glycerol, [U-$^{13}C_3$]glycerol, [3-^{13}C]lactate, or [U-$^{13}C_3$]lactate can be computed to yield the contribution of GNG to glucose production, provided that three conditions are met in all cells that synthesize glucose. First, the enrichments of the two triose phosphates are practically equal. Second, the enrichment of triose phosphates in all these cells is constant. Third, the contribution of the labeled substrate to GNG in all these cells is constant.

Neese et al (102, 103) and Péroni et al (107, 108) infused rats starved for two days with [2-^{13}C]glycerol, measured the MID of plasma glucose, and calculated contributions of GNG to glucose production (f) that were close to 100%. This was expected, since livers from rats starved for two days have negligible glycogen concentration. Thus GNG should contribute 100% of glucose production. In contrast, Landau et al (73) infused [U-$^{13}C_3$]glycerol to 60-h fasted humans and calculated an f of about 60%. Previs et al (110) perfused livers from rats starved two days with [U-$^{13}C_3$]glycerol or with [2-^{13}C]glycerol and found f values of about 75%. They also infused live rats with [U-$^{13}C_3$]glycerol and measured f of about 75%.

Landau et al (73) hypothesized that the concentration of glycerol decreases markedly as blood goes through the liver lobule. This would result in a progressive decrease in the labeling of triose phosphates from the periportal to the pericentral region of the lobule. As a consequence, the labeling of glucose would not be uniform, and artifactually low values of f would be calculated. In rat livers perfused with a physiological glycerol concentration (0.1 mM), Previs et al (110) measured a 90% decrease in glycerol concentration in a single pass of the perfusate through the liver. This observation was confirmed in human (76) and dog experiments (111) in which the balance of glycerol was measured across the splanchnic bed and across the liver, respectively. The findings of Neese et al (102, 103) and Péroni et al (107, 108) contrast with those of Landau et al (73) and Previs et al (110). This may result from the fact that the first authors infused fairly large amounts of [2-^{13}C]glycerol, which decreased the concentration gradient across the liver. Previs et al (110) found that f increased from 75% to 85% to 92% when the concentration of glycerol in liver perfusate was increased from 0.1 to 0.5 to 1.5 mM, respectively.

To avoid a transhepatic gradient of glycerol concentration, Previs et al (109) incubated hepatocytes from rats fasted for two days in medium into which glycerol, lactate, and pyruvate were infused with infusion of glycerol/(lactate + pyruvate) at ratios ranging from 3.6 to 0.22. Either glycerol or lactate and pyruvate were ^{13}C labeled. Substrate concentrations remained (nearly) physiological: lactate 1 mM, pyruvate 0.08–0.2 mM, glycerol 0.05–0.3 mM. When

all substrates were ^{13}C labeled, *f* was 97%. As the infusion rate ratio decreased, *f* measured with [^{13}C]glycerol decreased from 95% to 78%, while *f* measured with [^{13}C]lactate plus [^{13}C]pyruvate increased from 76% to 93%. Similar data were obtained when the substrates were labeled on one or on all carbons.

In the intact liver, periportal and pericentral hepatocytes are in contact with very different glycerol concentrations (76, 110, 111). In contrast, the hepatocytes incubated by Previs et al (109) were all in contact with the same substrate concentrations and enrichments. The apparent variations in *f* measured in these total hepatocyte incubations show that the enrichment of triose phosphates is not equal in all cells. Since isolated periportal and pericentral hepatocytes have similar glycerol kinase activity (109), the low *f* values may result from differences in PEP-carboxykinase activity between periportal and pericentral hepatocytes (56). In vivo, the zonation of glycerol metabolism by substrate exhaustion (110) is likely to contribute to the heterogeneity of glucose labeling. At this stage, there is still major disagreement between the above authors regarding the suitability of labeled glycerol for tracing GNG in vivo.

Very recently, Tayek and Katz (121) presented another technique for measuring GNG. They infused [U-$^{13}C_6$]glucose and measured the accumulation of M1, M2, and M3 glucose, as well as M1, M2, and M3 lactate in plasma. From these MID, they calculated the contribution of GNG to glucose production and the rate of Cori cycling. This new technique has not yet been evaluated.

Protein Synthesis

Hellerstein et al's MIDA technique has been applied to measurement of protein synthesis in animals infused with labeled amino acids. Preliminary reports (106) describe measurement of the MID of protein fragments by electrospray-MS and the calculation of fractional synthesis. The validation of this promising technique requires a direct comparison between the enrichment of the labeled amino acid calculated by MIDA of protein fragments and that measured on the tRNA.

CONCLUSIONS

The number and diversity of reports we reviewed reflect the tremendous development of techniques and studies based on MID measurements over the past six years. These techniques open new avenues on the regulation of metabolic pathways and on the synthesis of polymeric molecules. Because of the rapid pace of development, the interpretation of data required new mathematical tools that are still being refined. The limitations of these powerful techniques, particularly with regard to the synthesis of polymeric molecules, are slowly emerging. MID analysis may be applicable only to problems in which strict

conditions of validity can be demonstrated. The investigators who pioneered these techniques must be credited for their inventiveness and for great leaps in knowledge and understanding.

ACKNOWLEDGMENTS

This work was supported by grants from the National Institutes of Health (DKK35543 to HB, DK45164 to JKK) and from the Medical Research Council of Canada (MA9575 to CDR).

Literature Cited

1. Aarsland A, Chinkes DL, Wolfe R. 1996. Contributions of *de novo* synthesis of fatty acids and lipolysis to VLDL–triglyceride secretion during prolonged hyperglycemia/hyperinsulinemia in normal man. *J. Clin. Invest.* 98:1–10

1a. Aarsland A, Wolfe RR, Chinkes D. 1997. Hepatic and whole body fat synthesis in humans during carbohydrate overfeeding. *Am. J. Clin. Nutr.* 65:1774–82

2. Ajie HO, Connor MJ, Bassilian S, Bergner EA, Byerley LO, et al. 1995. *In vivo* study of the biosynthesis of long-chain fatty acids using deuterated water. *Am. J. Physiol.* 269:E247–52

3. Avogaro A, Doria A, Gnudi L, Carrara A, Duner E, Brocco E, et al. 1992. Forearm ketone body metabolism in normal and in insulin-dependent diabetic patients. *Am. J. Physiol.* 263:E261–67

4. Avogaro A, Nosadini R, Bier DM, Cobelli C, Toffolo G, et al. 1990. Ketone body kinetics *in vivo* using simultaneous administration of acetoacetate and 3-hydroxybutyrate labeled with stable isotopes. *Acta Diabetol. Lat.* 27:41–51

5. Berthold HK, Crain PF, Gouni I, Reeds PJ, Klein PD. 1995. Evidence for incorporation of intact dietary pyrimidine (but not purine) nucleosides into hepatic RNA. *Proc. Natl. Acad. Sci. USA* 92:10123–27

6. Berthold HK, Hachey DL, Reeds PJ, Thomas OP, Hoeksema S, Klein PD. 1991. Uniformly ^{13}C-labeled algal protein used to determine amino acid essentiality *in vivo*. *Proc. Natl. Acad. Sci. USA* 88:8091–95

7. Berthold HK, Reeds PJ, Klein PD. 1995. Isotopic evidence for the differential regulation of arginine and proline synthesis in man. *Metabolism* 44:466–73

8. Berthold HK, Wykes LJ, Jahoor F, Klein PD, Reeds PJ. 1994. The use of uniformly labeled substrates and mass isotopomer analysis to study intermediary metabolism. *Proc. Nutr. Soc.* 53:345–54

9. Beylot M, Soloviev MV, David F, Landau BR, Brunengraber H. 1995. Tracing hepatic gluconeogenesis relative to citric acid cycle activity *in vitro* and *in vivo*:Comparisons in the use of [3-^{13}C]lactate, [2-^{13}C]acetate and α-keto[3-^{13}C]isocaproate. *J. Biol. Chem.* 270: 1509–14

10. Biolo G, Tessari P, Inchiostro S, Bruttomesso D, Foncher C, et al. 1992. Leucine and phenylalanine kinetics during mixed meal ingestion: a multiple tracer approach. *Am. J. Physiol.* 262: E455–63

11. Boza JJ, Jahoor F, Reeds PJ. 1996. Ribonucleic acid nucleotides in maternal and fetal tissues derive almost exclusively from synthesis *de novo* in pregnant mice. *J. Nutr.* 126:1749–58

12. Breuer O, Bjorkhelm I. 1995. Use of an $^{18}O_2$ inhalation technique and mass isotopomer distribution analysis to study oxygenation of cholesterol in the rat. Evidence for *in vivo* formation of 7-oxo-, 7 beta-hydroxy-, 24 hydroxy-, and 25-hydrocholesterol. *J. Biol. Chem.* 270:20278–84

13. Brosnan JT, Brosnan ME, Charron R, Nissim I. 1996. A mass isotopomer study of urea and glutamine synthesis from ^{15}N-labeled ammonia in the

perfused rat liver. *J. Biol. Chem.* 271:16199–207
14. Brunengraber H, Boutry M, Lowenstein JM. 1978. Fatty acid, 3-β-hydroxysterol, and ketone synthesis in the perfused rat liver. II. Effects of (-)-hydroxycitrate and oleate. *Eur. J. Biochem.* 82:373–84
15. Brunengraber DZ, Yang D, Beylot M, Diraison F, Brunengraber H, et al. 1997. Measurement of deuterium enrichment of water by isotopic exchange with [U-^{13}C] acetone and GC-MS. *FASEB J.* 11:A518
16. Carver JD, Walker WA. 1995. The role of nucleotides in human nutrition. *J. Nutr. Biochem.* 6:58–72
17. Castillo L, Chapman TE, Yu Y-M, Ajami A, Burke JT, Young VR. 1993. Dietary arginine uptake by the splanchnic region in adult humans. *Am. J. Physiol.* 265:E532–39
18. Chatham JC, Forder JR, Glickson JD, Chance EW. 1995. Calculation of absolute metabolic flux and the elucidation of the pathways of glutamate labeling in perfused rat heart by ^{13}C NMR spectroscopy and non linear least quares analysis. *J. Biol. Chem.* 270:7999–8008
19. Chinkes DL, Aarsland A, Rosenblatt J, Wolfe RR. 1996. A comparison of mass isotopomer dilution methods used to compute production of VLDL fatty acids *in vivo* in human subjects. *Am. J. Physiol.* 271:E373–83
20. Cline GW, Shulman GI. 1995. Mass and positional isotopomer analysis of glucose metabolism in periportal and pericentral hepatocytes. *J. Biol. Chem.* 270:28062–67
21. Cobelli C, Toffolo G, Bier DM, Nosadini R. 1987. Models to interpret kinetic data in stable isotope tracer studies. *Am. J. Physiol.* 253:E551–64
22. Cohen DM, Bergman RN. 1994. Prediction of positional isotopomers of the citric acid cycle: the syntactic approach. *Am. J. Physiol.* 266:E341–50
23. Comte B, Des Rosiers C. 1997. Contribution of pyruvate carboxylation and decarboxylation to citrate formation in the perfused rat heart. Direct assessment from the ^{13}C-labeling of effluent citrate. *J. Biol. Chem.* (in revision)
24. Comte B, Vincent G, Jetté M, Des Rosiers C. 1997. Importance of pyruvate carboxylation in the perfused rat heart. A ^{13}C-mass isotopomer study. *J. Biol. Chem.* (in revision)
25. Coppack SW, Jensen MD, Miles JM. 1994. *In vivo* regulation of lipolysis in humans. *J. Lipid Res.* 35:177–93
26. Crabb DW, Yount EA, Harris RA. 1981. The metabolic effects of dichloroacetate. *Metabolism* 30:1024–39
27. Des Rosiers C, Di Donato L, Comte B, Laplante A, Marcoux C, et al. 1995. Isotopomer analysis of citric acid cycle and gluconeogenesis in rat liver: Reversibility of isocitrate dehydrogenase and involvement of ATP-citrate lyase in gluconeogenesis. *J. Biol. Chem.* 270:10027–36
28. Des Rosiers C, Fernandez CA, David F, Brunengraber H. 1994. Reversibility of the mitochondrial isocitrate dehydrogenase reaction in the perfused rat liver: Evidence from isotopomer analysis of citric acid cycle intermediates. *J. Biol. Chem.* 269:27179–82
29. Des Rosiers C, Landau BR, Brunengraber H. 1990. Interpretation of isotopomer patterns in tracing glycogen synthesis and glucose recycling using [$^{13}C_6$]glucose. *Am. J. Physiol.* 259:E757–62
30. Des Rosiers C, Montgomery JA, Desrochers S, Garneau M, David F, et al. 1988. Interference of 3-hydroxyisobutyrate with measurements of ketone body concentration and isotopic enrichment by gas chromatography-mass spectrometry. *Anal. Biochem.* 173:96–105
31. Des Rosiers C, Montgomery JA, Garneau M, David F, Mamer OA, et al. 1990. Pseudoketogenesis in hepatectomized dogs. *Am. J. Physiol.* 258:E519–28
32. Di Donato L, Des Rosiers C, Montgomery JA, David F, Garneau M, et al. 1993. Rates of gluconeogenesis and citric acid cycle in perfused livers, assessed from the mass spectrometric assay of the [^{13}C]labeling pattern of glutamate. *J. Biol. Chem.* 268:4170–80
33. Diraison F, Pachiaudi C, Beylot M. 1996. *In vivo* measurement of plasma cholesterol and fatty acid synthesis with deuterated water:determination of the average number of deuterium atoms incorporated. *Metabolism* 45:817–21
34. Diraison F, Pachiaudi C, Beylot M. 1997. Measuring lipogenesis and cholesterol synthesis in humans with deuterated water: use of simple gas chromatographic/mass spectrometric techniques. *J. Mass Spectrom.* 32:81–86
35. Ekberg K, Chandramouli V, Kumaran K, Schumann WC, Wahren J, et al. 1995. Gluconeogenesis and glucuronidation in liver *in vivo* and the heterogeneity of hepatocyte function. *J. Biol. Chem.* 270:21715–17
36. Endemann G, Goetz PG, Edmond J,

Brunengraber H. 1982. Lipogenesis from ketone bodies in the isolated perfused rat liver; evidence for the cytosolic activation of acetoacetate. *J. Biol. Chem.* 257:3434–40

37. Endemann G, Goetz PG, Tomera JF, Rand WM, Desrochers S, Brunengraber H. 1987. Lipogenesis from ketone bodies in the perfused rat liver: effects of acetate and ethanol. *Biochem. Cell Biol.* 65:989–96
38. Fernandez CA, Des Rosiers C. 1995. Modeling of liver citric acid cycle and gluconeogenesis based on ^{13}C mass isotopomer distribution analysis of intermediates. *J. Biol. Chem.* 270:10037–42
39. Fernandez CA, Des Rosiers C, Previs SF, David F, Brunengraber H. 1996. Correction of ^{13}C mass isotopomer distributions for natural stable isotope abundance. *J. Mass Spectrom.* 31:255–62
40. Féry F, Balasse EO. 1985. Ketone body production and disposal in diabetic ketosis. A comparison with fasting ketosis. *Diabetes* 34:326–32
41. Fink G, Desrochers S, Des Rosiers C, Garneau M, David F, et al. 1988. Pseudoketogenesis in the perfused rat heart. *J. Biol. Chem.* 263:18036–42
42. Hachey DL, Patterson BW, Reeds PJ, Elsas LJ. 1991. Isoptopic determination of organic keto acid pentafluorobenzyl esters in biological fluids by negative chemical ionization gas chromatography/mass spectrometry. *Anal. Chem.* 63:919–23
43. Hazey JW, Powers L, Previs SF, Yang D, David F, et al. 1997. Tracing gluconeogenesis with deuterated water:measurement of low deuterium enrichments on carbons 6 and 2 of glucose. *Anal. Biochem.* 248:158–67
44. Hellerstein MK. 1991. Relationship between precursor enrichment and ratio of excess M2/excess M1 isotopomer frequencies in a secreted polymer. *J. Biol. Chem.* 266:10920–24
45. Hellerstein MK, Christiansen M, Kaempfer S, Kletke C, Wu K, et al. 1991. Measurement of *de novo* hepatic lipogenesis in humans using stable isotopes. *J. Clin. Invest.* 87:1841–52
46. Hellerstein MK, Greenblatt DJ, Munro HN. 1986. Glucuronides as noninvasive probes of intrahepatic metabolism: pathways of glucose entry into compartmentalized hepatic UDP–glucose pools during glycogen accumulation. *Proc. Natl. Acad. Sci. USA* 83:7044–48
47. Hellerstein MK, Kaempfer S, Reid JS, Wu K, Shackelton CH. 1995. Rate of glucose entry into hepatic uridine diphosphoglucose by the direct pathway in fasted and fed states in normal humans. *Metabolism* 44:172–82
48. Hellerstein MK, Kletke C, Kaempfer S, Wu K, Shackelton CH. 1991. Use of mass isotopomer distributions in secreted lipids to sample lipogenic acetyl–CoA pool in humans. *Am. J. Physiol.* 261:E479–86
49. Hellerstein MK, Neese RA. 1992. Mass isotopomer distribution analysis:a technique for measuring biosynthesis and turnover of polymers. *Am. J. Physiol.* 263:E988–1001
50. Hellerstein MK, Neese RA, Schwarz JM. 1993. Model for measuring absolute rates of hepatic *de novo* lipogenesis and reesterification of free fatty acids. *Am. J. Physiol.* 265:E814–20
51. Hellerstein MK, Schwartz JM, Neese RA. 1996. Regulation of hepatic *de novo* lipogenesis in humans. *Annu. Rev. Nutr.* 16:523–57
52. Hellerstein MK, Wu K, Kaempfer S, Kletke C, Shackelton CH. 1991. Sampling the lipogenic hepatic acetyl-CoA pool *in vivo* in the rat. Comparison of xenobiotic probe to values predicted from isotopomeric distribution in circulating lipids and measurement of lipogenesis and acetyl-CoA dilution. *J. Biol. Chem.* 266:10912–19
53. Hochachka PW, Storey KB. 1975. Metabolic consequences of diving in animals and man. *Science* 187:613–21
54. Jones PJH, Schoeller DA. 1990. Evidence for diurnal periodicity in human cholesterol synthesis. *J. Lipid Res.* 31:667–73
55. Jungas RL. 1965. Fatty acid synthesis in adipose tissue incubated in tritiated water. *Biochemistry* 7:3708–17
56. Jungerman K, Thurman RG. 1992. Hepatocyte heterogeneity in the metabolism of carboydrates. *Enzyme* 46:33–58
57. Kalderon B, Gopher A, Lapidot A. 1986. Metabolic pathways leading to liver glycogen repletion *in vivo*, studied by GCMS and NMR. *FEBS Lett.* 204:29–32
58. Kalderon B, Korman SH, Gutman A, Lapidot A. 1989. Glucose recycling and production in glycogenosis type I and III:stable isotope technique study. *Am. J. Physiol.* 257:E346–53
59. Kalderon B, Lapidot A, Korman SH, Gutman A. 1988. Glucose recycling and production in children with glycogen storage disease type I, studied by gas chromatography/mass spectrometry and [U-^{13}C]glucose. *Biomed. Environ. Mass Spectrom.* 16:305–8

60. Kalhan SC. 1996. Stable isotope tracers for studies of glucose metabolism. *J. Nutr.* 126:S362–69
61. Kassel DB, Glerum M, Robinson BH, Sweely CC. 1989. Determination of [U-^{13}C]glucose turnover into various metabolic pools for the differential diagnosis of lactic acidemias. *Anal. Biochem.* 176:382–89
62. Katz J, Lee WNP. 1991. Application of mass isotopomer analysis for determination of pathways of glycogen synthesis. *Am. J. Physiol.* 261:E332–36
63. Katz J, Lee WNP, Wals PA, Bergner EA. 1989. Studies of glycogen synthesis and the Krebs cycle by mass isotopomer analysis with [U-^{13}C]glucose in rats. *J. Biol. Chem.* 264:12994–3001
64. Katz J, Wals P, Lee WNP. 1993. Isotopomer studies of gluconeogenesis and the Krebs cycle with ^{13}C-labeled lactate. *J. Biol. Chem.* 268:25509–21
65. Katz J, Wals PA, Lee WNP. 1991. Determination of pathways of glycogen synthesis and the dilution of the three-carbon pool with [U-^{13}C]glucose. *Proc. Natl. Acad. Sci. USA* 88:2103–7
66. Kelleher JK. 1995. Isotopomer spectral analysis: Encountering variable pool size and *enrichment. Ann. Biomed. Eng.* 23:S72 (Abstr.)
67. Kelleher JK, Kharroubi AT, Aldaghles TA, Shambat IB, Kennedy KA, et al. 1994. Isotopomer spectral analysis of cholesterol synthesis:applications in human hepatoma cells. *Am. J. Physiol.* 266:E384–95
68. Kelleher JK, Masterson TM. 1992. Model equations for condensation biosynthesis using stable isotopes and radioisotopes. *Am. J. Physiol.* 262:E118–25
69. Keshen T, Miller R, Jahoor F, Jaksic T, Reeds PJ. 1997. Glucose production and gluconeogenesis are negatively related to body weight in mechanically-ventilated very-low-birth-weight neonates. *Pediatr. Res.* 41:132–38
70. Kharroubi AK, Masterson TM, Aldaghlas TA, Kennedy KA, Kelleher JK. 1992. Isotopomer spectral analysis estimates of trigyceride fatty acid synthesis in 3T3 L_1 cells. *Am. J. Physiol.* 263:E667–75
71. Landau BR. 1993. Estimating gluconeogenic rates in NIDDM. *Adv. Exp. Med. Biol.* 334:209–20
72. Landau BR. 1986. A potential pitfall in the use of isotopes to measure ketone body production. *Metabolism* 35:94–95
73. Landau BR, Fernandez CA, Previs SF, Ekberg K, Chandramouli V, et al. 1995. A limitation in the use of mass isotopomer distributions to measure gluconeogenesis in fasting humans: Hepatic heterogeneity in glycerol metabolism. *Am. J. Physiol.* 269:E18–E26
74. Landau BR, Wahren J, Chandramouli V, Schumann WC, Ekberg K, et al. 1996. Contributions of gluconeogenesis to glucose production in the fasted state. *J. Clin. Invest.* 98:378–85
75. Landau BR, Wahren J, Chandramouli V, Schumann WC, Ekberg K, Kalhan SC. 1995. Use of ^2H_2O for estimating rates of gluconeogenesis. *J. Clin. Invest.* 95:172–78
76. Landau BR, Wahren J, Previs SF, Ekberg K, Chandramouli V, Brunengraber H. 1996. Glycerol production and utilization in humans:sites and quantitation. *Am. J. Physiol.* 271:E1110–17
77. Lapidot A, Gopher A. 1994. Cerebral metabolic compartmentation. Estimation of glucose flux via pyruvate carboxylase/pyruvate dehydrogenase by ^{13}C NMR isotopomer analysis of D-[U-^{13}C]glucose metabolites. *J. Biol. Chem.* 269:27198–208
78. Laplante A, Vincent G, Poirier M, Des Rosiers C. 1997. Effects and metabolism of fumarate in the perfused rat heart. A ^{13}C-mass isotopomer study. *Am. J. Physiol.* 272:E74–82
79. Lee WNP. 1996. Stable isotopes and mass isotopomer study of fatty acid and cholesterol synthesis: a review of the MIDA approach. In *Dietary Fats, Lipids, Hormones and Tumorogenesis,* ed. D Heber, D Kritchevsky, pp. 95–114. New York: Plenum
80. Lee WNP. 1993. Appendix. Analysis of tricarboxylic acid cycle using mass isotopomer ratios. *J. Biol. Chem.* 268: 25522–26
81. Lee WNP, Bassilian S, Ajie H, Schoeller D, Edmond J, et al. 1994. *In vivo* measurement of fatty acids and cholesterol synthesis using D_2O and mass isotopomer analysis. *Am. J. Physiol.* 266:E699–708
82. Lee WNP, Bassilian S, Guo ZK, Schoeller D, Edmond J, et al. 1994. Measurement of fractional lipid synthesis using deuterated water (^2H_2O) and mass isotopomer analysis. *Am. J. Physiol.* 266:E372–83
83. Lee WNP, Bergner EA, Guo ZK. 1992. Mass isotopomer pattern and precursor-product relationship. *Biol. Mass Spectrom.* 21:114–22
84. Lee WNP, Byerly LO, Bassilian S, Ajie HO, Clark I, et al. 1995. Isotopomer study of lipogenesis in human hepatoma

cells in culture: contribution of carbon and hydrogen atoms from glucose. *Anal. Biochem.* 226:100–12

85. Lee WNP, Byerley LO, Bergner EA, Edmond J. 1991. Mass isotopomer analysis: theoretical and practical considerations. *Biol. Mass Spectrom.* 20:451–58
86. Lee WNP, Sorou S, Bergner EA. 1991. Glucose isotope, carbon recycling, and gluconeogenesis using [U-^{13}C]glucose and mass isotopomer analysis. *Biochem. Med. Metab. Biol.* 45:298–309
87. Lee WNP. 1989. Appendix. Analysis of mass isotopomer data. *J. Biol. Chem.* 264:13002–4
88. Leitch CA, Jones PJH. 1993. Measurement of human lipogenesis using deuterium incorporation. *J. Lipid Res.* 34:157–63
89. Lewandowski EG, Johnston DL. 1990. Reduced substrate oxidation in postischemic myocardium:^{13}C and ^{31}P NMR analysis. *Am. J. Physiol.* 258:H1357–65
90. Lin YY, Cheng WB, Wright CE. 1993. Glucose metabolism in mammalian cells as determined by mass isotopomer analysis. *Anal. Biochem.* 209:267–73
91. Lowenstein JM. 1971. Effect of (-)-hydroxycitrate on fatty acid synthesis by rat liver *in vivo*. *J. Biol. Chem.* 246:629–32
92. Lowenstein JM, Brunengraber H, Wadke M. 1975. Measurement of rates of lipogenesis with deuterated and tritiated water. *Methods Enzymol.* 35:279
93. Magnusson I, Chandramouli V, Schumann WC, Kumaran K, Wahren J, et al. 1987. Quantitation of the pathways of hepatic glycogen formation in ingesting a glucose load. *J. Clin. Invest.* 80:1748–54
94. Magnusson I, Schumann WC, Bartsch GE, Chandramouli V, Kumaran K, et al. 1991. Noninvasive tracing of Krebs cycle metabolism in liver. *J. Biol. Chem.* 266:6975–84
95. Malloy CR, Sherry AD, Jeffrey FMH. 1990. Analysis of tricarboxylic acid cycle of the heart using ^{13}C isotope isomers. *Am. J. Physiol.* 259:H987–95
96. Malloy CR, Thompson JR, Jeffrey FMH, Sherry AD. 1990. Contribution of exogenous substrates to acetyl conenzyme A: measurement of ^{13}C NMR under non-steady state conditions. *Biochemistry* 29:6756–61
97. Mamer OA. 1988. Measurement of urinary lactic, 3-hydroxybutyric, pyruvic and acetoacetic acids in a single analysis using selcted ion monitoring and stable isotope labeling techniques. *Biomed. Environ. Mass Spectrom.* 15:57–62
98. Marchini JS, Castillo L, Chapman TE, Vogt JA, Ajami A, et al. 1993. Phenylalanine conversion to tyrosine: comparative determination with L-[ring-$^{2}H_5$]phenlylalanine and L-[1-^{13}C]phenylananine as tracers in man. *Metabolism* 42:1316–22
99. Martin G, Chauvin MF, Dugelay S, Baverel G. 1994. Non-steady state model applicable to NMR studies for calculating flux rates in glycolysis, gluconeogenesis, and citric acid cycle. *J. Biol. Chem.* 269:26034–39
100. Neese RA, Benowitz NL, Hoh R, Faix D, LaBua A, et al. 1994. Metabolic interactions between surplus dietary energy intake and cigarette smoking or its cessation. *Am. J. Physiol.* 267:E1023–34
101. Neese RA, Faix D, Kletke C, Wu K, Shackleton CHL, et al. 1993. Measurement of endogenous synthesis of serum cholesterol *in vivo* rats and humans using mass isotopomer distribution analysis (MIDA). *Am. J. Physiol.* 264:E136–47
102. Neese RA, Hellerstein MK. 1995. Appendix. Calculations for gluconeogenesis by MIDA. *J. Biol. Chem.* 270:14464–66
103. Neese RA, Schwartz JM, Faix D, Turner SM, Vu D, et al. 1995. Gluconeogenesis and intrahepatic triose phosphate flux in response to fasting or substrate loads. *J. Biol. Chem.* 270:14452–63
104. Nieto R, Calder AG, Anderson SE, Lobley GE. 1996. Method for the determination of $^{15}NH_3$ enrichment in biological samples by gas chromatography/electron impact ionization mass spectrometry. *J. Mass. Spectrom.* 31:289–94
105. Nissim I, Yudkoff M, Yang W, Terwilliger T, Segal S. 1981. Gas chromatography-mass spectrometry determination of ^{15}N ammonia enrichment in blood and urine. *Anal. Biochem.* 114:125–30
106. Papageorgopoulos C, Caldwell KA, Siler SO, Neese RA, Hellerstein MK. 1995. Measurement of muscle myosin synthesis by mass isotopomer distribution analysis (MIDA). *FASEB J.* 9:A864
107. Péroni O, Large V, Beylot M. 1995. Measuring gluconeogenesis with [2-^{13}C]glycerol and mass isotopomer distribution analysis of glucose. *Am. J. Physiol.* 269:E516–23
108. Péroni O, Large V, Odeon M, Beylot M. 1996. Measuring glycerol turnover, gluconeogenesis from glycerol, and total gluconeogenesis with [2-^{13}C]glycerol:role of

the infusion-sampling mode. *Metabolism* 45:897–901

109. Previs SF, Hallowell PT, David F, Neimanis K, Brunengraber H. 1997. Labeling heterogeneity of glucose in hepatocytes incubated with glycerol, lactate and pyruvate: Evaluation of limitations and hepatic zonation of glycerokinase activity. *FASEB J.* 11:A436 (Abstr. 2525)
110. Previs SF, Fernandez CA, Yang D, Soloviev MV, David F, Brunengraber H. 1995. Limitations of mass isotopomer distribution analysis of glucose to study gluconeogenesis: Substrate cycling between glycerol and triose phosphates in liver. *J. Biol. Chem.* 270:19806–15
111. Previs SF, Martin SK, Hazey JW, Soloviev MV, Keating AP, et al. 1996. Contributions of liver and kidneys to glycerol production and utilization in the dog. *Am. J. Physiol.* 271:E1118–24
112. Reszko AE, Yang D, Brunengraber H. 1997. Assay of the concentration and stable isotopic enrichment of formaldehyde by GC-MS of hexamethylenetetramine (HMT). *FASEB J.* 11:A385 (Abstr. 2227)
113. Roe CR, Coates PM. 1989. Acyl-CoA dehydrogenase deficiencies. In *The Metabolic Basis of Inherited Disease* I, ed. CR Scriver, pp. 889–931. New York: McGraw-Hill
114. Rosenblatt J, Chinkes D, Wolfe M, Wolfe RR. 1992. Stable isotope tracer analysis by GC-MS, including quantification of isotopomer effects. *Am. J. Physiol.* 263:E584–96
115. Rother KI, Schwenk WF. 1995. Hepatic glycogen accurately reflected by acetaminophen glucuronide in dogs refed after fasting. *Am. J. Physiol.* 269:E766–73
116. Sazanov LA, Jackson JB. 1994. Proton-translocating transhydrogenase and NAD- and NADP-linked isocitrate dehydrogenase operate in a substrate cycle which contributes to fine regulation of tricarboxylic acid cycle activity in mitochondria. *FEBS Lett.* 344:109–16
117. Schoenheimer R, Rittenberg DJ. 1937. Deuterium as an indicator in the study of intermediary metabolism. *J. Biol. Chem.* 114:381–96
118. Schumann WC, Magnusson I, Chandramouli V, Kumaran K, Wahren J, et al. 1991. Metabolism of [2-^{14}C]acetate and its use in assessing hepatic Krebs cycle activity and gluconeogenesis. *J. Biol. Chem.* 266:6985–90
119. Seeman JI, Paine JB. 1992. Isotopomers, isotopologs. *Chem. Eng. News* 70:2
120. Strong JM, Upton DK, Anderson LW, Monks A, Chisena CA, et al. 1988. A novel approach to the analysis of the mass spectrally assayed stable isotope-labeling experiments. *J. Biol. Chem.* 260:4276–81
121. Tayek J, Katz J. 1996. Glucose production, recycling, and gluconeogenesis in normal and diabetics: a mass isotopomer [U-^{13}C]glucose study. *Am. J. Physiol.* 270:E709–17
122. Tserng KY, Jin SJ. 1991. Metabolic conversion of dicarboxylic acids to succinate in rat liver homogenates. A stable isotope tracer study. *J. Biol. Chem.* 266:2924–29
123. Vogt JA, Chapman TE, Wagner DA, Young VR, Burke JF. 1993. Determination of the isotope enrichment of one or a mixture of two stable labeled tracers of the same compound using the complete isotopomer distribution of an ion fragment; theory and application to *in vivo* human tracer studies. *Biol. Mass. Spectrom.* 22:600–12
124. Vogt JA, Fischman AJ, Kempf M, Yu YM, Tompkins RG, Burke JF. 1994. A general model for tricarboxlylic acid cycle with use of [^{13}C]glutamate isotopomer measurements. *Am. J. Physiol.* 266:E1012–22
125. Wada F, Usami M. 1977. Studies on fatty acid omega-oxidation. Antiketogenic effect and gluconeogenicity of dicarboxylic acids. *Biochim. Biophys. Acta* 487:361–68
126. Wadke M, Brunengraber H, Lowenstein JM, Dolhun JJ, Arsenault GP. 1973. Fatty acid synthesis by the liver perfused with deuterated water and tritiated water. *Biochemistry* 12:2619–24
127. Weiss RG, Chacko VP, Glickson JD, Gerstenblith G. 1989. Comparative ^{13}C and ^{31}P NMR assessment of altered metabolism during graded reductions in coronary flow in intact rat hearts. *Proc. Natl. Acad. Sci. USA* 86:6426–30
128. Wolfe RR. 1992. *Radioactive and Stable Isotope Tracers in Biomedicine: Principles and Practice of Kinetic Analysis.* New York: Wiley-Liss
129. Deleted in proof.
130. Wykes LJ, Jahoor F, Reeds PJ, Fraser ME, DelRasio M. 1994. Serine and alanine derive from different three-carbon presursor pools: Evidence from mass isotopomer-analysis. *FASEB J.* 8:A462 (Abstr. #2676)
131. Yang D, Hazey JH, Powers L, David F, Singh J, et al. 1997. GC-MS assay of low concentration and stable isotopic enrichment of plasma ammonia. *FASEB J.* 11:A267 (Abstr. 1552)

132. Yang D, Previs SF, Fernandez CA, Dugelay S, Soloviev MV, et al. 1996. Noninvasive probing of liver citric acid cycle intermediates with phenylacetylglutamine. *Am. J. Physiol.* 270:E882–89
133. Yudkoff M, Nelson D, Daikhin Y, Erecinska M. 1994. Tricarboxylic acid cycle in rat brain synaptosomes. *J. Biol. Chem.* 269:27414–20
134. Zhang Y, Agarwal KC, Beylot M, Soloviev MV, David F, et al. 1994. Non-homogeneous labeling of liver extramitochondrial acetyl-CoA: Implications for the probing of lipogenic acetyl-CoA via drug acetylation and for the production of acetate by the liver. *J. Biol. Chem.* 269:11025–29
135. Zhang Y, Agarwal KC, Beylot, M, Soloviev MV, David F, et al. 1993. Assay of the acetyl-CoA probe acetylsulfamethoxazole and of sulfamethoxazole by gas chromatography-mass spectrometry. *Anal. Biochem.* 212:481–86